

Unclassified

Zameer Hasan

Grant # F49620-96-1-0347

July 2002

Temple University
Department of Physics
Barton Hall, 1900 N. 13th Street
Philadelphia, PA 19122

Unclassified

20020903 034

Unclassified

Ultra-High Density Spectral Storage Materials

Zameer Hasan

Grant # F49620-96-1-0347

July 2002

Temple University
Department of Physics
Barton Hall, 1900 N. 13th Street
Philadelphia, PA 19122

Unclassified

REPORT DOCUMENTATION PAGE

AFRL-SR-AR-TR-02-

0257

Public reporting burden for this collection of information is estimated to average 1 hour per response, including the time for reviewing data needed, and completing and reviewing this collection of information. Send comments regarding this burden estimate or any other aspect of this burden to Department of Defense, Washington Headquarters Services, Directorate for Information Operations and Reports (0704-4302). Respondents should be aware that notwithstanding any other provision of law, no person shall be subject to any penalty for fail valid OMB control number. PLEASE DO NOT RETURN YOUR FORM TO THE ABOVE ADDRESS.

1. REPORT DATE (DD-MM-YYYY) 18-07-2002		2. REPORT TYPE Final		3. DATES COVERED (From - To) July 1996-December 2001	
4. TITLE AND SUBTITLE Ultra-High Density Spectral Storage Materials				5a. CONTRACT NUMBER F49620-96-1-0347	
				5b. GRANT NUMBER	
				5c. PROGRAM ELEMENT NUMBER	
6. AUTHOR(S) Z. U. Hasan				5d. PROJECT NUMBER	
				5e. TASK NUMBER	
				5f. WORK UNIT NUMBER	
7. PERFORMING ORGANIZATION NAME(S) AND ADDRESS(ES) Temple University 1900 N. 13 th St. Philadelphia, PA 19122				8. PERFORMING ORGANIZATION REPORT NUMBER 2313659-7	
9. SPONSORING / MONITORING AGENCY NAME(S) AND ADDRESS(ES) U.S Air Force Office of Scientific Research NSWC, Cardrock Dr. 9500 MacArthur Blvd. Bethesda, MD 20817				10. SPONSOR/MONITOR'S ACRONYM(S) AFOSR	
				11. SPONSOR/MONITOR'S REPORT NUMBER(S)	
12. DISTRIBUTION / AVAILABILITY STATEMENT General/Public				APPROVED FOR PUBLIC RELEASE, DISTRIBUTION UNLIMITED	
13. SUPPLEMENTARY NOTES					
14. ABSTRACT This report deals with the development of solid-state materials for ultra-dense spectral storage. Being atomic scale storage, spectral storage has the potential of providing orders of magnitude denser memories than present day memories that depend on the bulk properties of the storage medium. Atomic and bulk properties of rare earth doped wide band gap semiconductors, particularly alkaline earth sulfides, have been tailored and a novel storage technique, power-gated holeburning, has been devised. It has been demonstrated that this combination of materials and method of storage allows for ultra-dense, fast, persistent, and rewriteable spectral memories. The improvement in performance parameters has been by orders of magnitude, and more importantly, all favorable characteristics of spectral storage have been combined in a single material, Magnesium Sulfide doped with Europium. It has been demonstrated that with the exception of low temperature operation, the performance of this materials matches or exceeds the standards of current commercial memories. On the basis of these investigations, it is apparent that almost all barriers to a commercially viable device based on spectral holeburning can be removed. Recommendations have been made for future research to increase the temperature of operation and to extend the range of spectral memories into the infrared.					
15. SUBJECT TERMS High Density Storage, Spectral Storage, Holeburning Memories, Spectral Memories, Rare Earth Power-Gated Holeburning, Photon-Gated Holeburning					
16. SECURITY CLASSIFICATION OF:			17. LIMITATION OF ABSTRACT	18. NUMBER OF PAGES 87	19a. NAME OF RESPONSIBLE PERSON Zameer U. Hasan
a. REPORT Unclassified	b. ABSTRACT Unclassified	c. THIS PAGE Unclassified			19b. TELEPHONE NUMBER (include area code) (215) 204-2733

Standard Form 298 (Rev. 8-98)
Prescribed by ANSI Std. Z39.18

Abstract

This report deals with the development of solid-state materials for ultra-dense spectral storage. Being atomic scale storage, spectral storage has the potential of providing orders of magnitude denser memories than present day memories that depend on the bulk properties of the storage medium. Atomic and bulk properties of rare earth doped wide band gap semiconductors, particularly alkaline earth sulfides, have been tailored and a novel storage technique, power-gated holeburning, has been devised. It has been demonstrated that this combination of materials and method of storage allows for ultra-dense, fast, persistent, and rewriteable spectral memories. The improvement in performance parameters has been by orders of magnitude, and more importantly, all favorable characteristics of spectral storage have been combined in a single material, Magnesium Sulfide doped with Europium. It has been demonstrated that with the exception of low temperature operation, the performance of this materials matches or exceeds the standards of current commercial memories. On the basis of these investigations, it is apparent that almost all barriers to a commercially viable device based on spectral holeburning can be removed. Recommendations have been made for future research to increase the temperature of operation and to extend the range of spectral memories into the infrared.

Contents

Abstract.....	iii
List of Figures.....	vi
Acknowledgements.....	viii
1. Summary.....	1
2. Personnel Supported.....	3
3. Introduction.....	5
4. Background and Experimental Methods.....	9
4.1 Homogeneous and Inhomogeneous Broadening in Solids.....	9
4.2 Photon-gated and Power-gated Holeburnings.....	10
4.3 Materials Selection.....	14
4.3.1 Structural Properties.....	14
4.3.2 Electronic Transitions in Rare Earth for High-Density Storage.....	15
4.3.3 Theoretical Estimate of 5d- Energy Levels.....	17
4.4 Material Designing and Processing.....	18
4.4.1 Microparticles of RE-Doped of II-VI Sulfides.....	18
4.4.2 Thin Film and Multi-Layer Structures.....	20
4.4.3 Multi-layer Thin Film Fabrication (LPVD).....	22
4.4.4 Nanoparticles by Quench Condensation of Laser Ablated Vapors.....	23
4.5 Material Characterization.....	23
4.5.1 Mössbauer Studies of $\text{Eu}^{2+}/\text{Eu}^{3+}$ Based Materials.....	25
4.5.2 Optical Characterization.....	25
4.6 Experimental Procedures for Optical Studies.....	25
4.6.1 Absorption, Emission and Excitation Setup.....	26
4.6.2 Pulsed Setup.....	26
4.6.3 High-Resolution Optical Holeburning Setup.....	28
4.7 Cryogenics.....	31
5. Results.....	34
5.1 Ultra-High Density Storage in $\text{MgS}:\text{Eu}^{2+}$	34

5.1.1 Mechanism of Holeburning.....	36
5.1.2 High Efficiency of Holeburning.....	37
5.1.3 Fast Writing.....	38
5.1.4 High Temperature Cycling and Storage of Data.....	38
5.1.5 Fast Optical Erasure.....	39
5.1.6 Low Photon Budget.....	42
5.1.7 Temperature Dependence.....	42
5.2 Ultra-High Density Storage in Thin Films.....	43
5.2.1 Ultra-High Density Storage in Multi-Layer, Multi-Center Structures.....	45
5.3 Mössbauer Studies.....	48
5.4 MgS:Eu Embedded in Different Hosts.....	48
5.4.1 High Density Holeburning in MgS:Eu in Polymers (PMMA).....	50
5.5 Holeburning in Nanoparticles.....	53
5.6 Temperature Dependence in Different Hosts.....	53
5.7 II-VI Materials Doubly Doped with Rare Earths.....	55
5.7.1 Holeburning in MgS:Eu,Sm.....	57
5.7.2 Holeburning in MgS:Eu,Ce.....	58
5.8 Al ₂ O ₃ :Ti ³⁺	58
6. Conclusion.....	62
7. Recommendations.....	64
8. References.....	66
9. Symbols, Abbreviations, Acronyms.....	70
10. Publications.....	71
11. Index.....	79

List of Figures

Figure 1.	Spectral Storage by Optical Holeburning.....	7
Figure 2.	Line Broadening in a Solid.....	11
Figure 3.	Photon-Gated Holeburning.....	11
Figure 4.	Power-Gated Holeburning.....	13
Figure 5.	Crystal Structure of MgS.....	16
Figure 6.	First Order Estimates of the Relevant Energy Levels.....	19
Figure 7.	Microparticles Experimental Setup.....	21
Figure 8.	LPVD Setup for Thin Film Deposition.....	21
Figure 9.	Parallel Optical Storage and Addressing in Multi-Center Multi-Layer Structure.....	24
Figure 10.	Nanoparticle Production.....	24
Figure 11.	The Excitation and Emission Setup.....	27
Figure 12.	Pulsed Setup for Lifetime, Fluorescence, Excitation, and Emission.....	29
Figure 13.	Pulse Train Synchronization.....	29
Figure 14A.	Experimental Setup for Photon-Gated and Power-Gated Holeburning.....	30
Figure 14B.	Experimental Setup for Nanosecond Holeburning.....	32
Figure 15.	High Density Holeburning in MgS:Eu ²⁺	35
Figure 16A.	Nanosecond Holeburning.....	40
Figure 16B.	Energy Levels and POGHB in MgS:Eu ²⁺	40
Figure 17A. & B.	Thermal Cycling of the Holes.....	41
Figure 18.	Temperature Dependence of the Holes in Powder.....	44
Figure 19A. & B.	Emission LPVD Thin Films.....	46
Figure 19C. & D.	Ultra Dense Holeburning in MgS:Eu and MgS:Eu + O Films.....	46
Figure 20.	Multi-Layer Structures and Their Parallel Addressing.....	47
Figure 21.	Ultra High Density Multi-Layer Storage.....	47
Figure 22.	Mössbauer Spectrum of MgS:Eu.....	49
Figure 23A.	Emission Spectra of MgS:Eu Microparticles in PMMA.....	51
Figure 23B.	Ultra-High Density Holeburning in MgS:Eu Embedded in PMMA.....	51

Figure 24.	Molecular Weight Dependence of the Linewidth.....	52
Figure 25.	Excitation Spectrum in MgS:Eu.....	54
Figure 26.	Persistent Spectral Holeburning in MgS:Eu.....	54
Figure 27.	Temperature Dependence of the Holewidth, MgS:Eu in PMMA.....	56
Figure 28.	Micro and Nanoparticles: Temperature Dependence of the Holewidth, MgS:Eu.....	56
Figure 29.	Holeburning in MgS:Eu + Ce.....	59
Figure 30	Holeburning in Al ₂ O ₃	61

Acknowledgement

The author would like to acknowledge the contribution of many students, post-doctoral fellows, and colleagues with whom he had the opportunity to work, in particular Levent Biyikli, Mikhail Solonenko, Milen Shishkov, Mohamed Aly, Sameh Dardona, Aras Konjhozic, and Robert Esposito worked for their doctoral theses. Drs. Jihsook Lee Park, Peter M. Macfarlane, S.M. Syed Ahmedyan, and Syed Moniruzzaman worked as post-doctoral fellows during the course of these investigations. He would also like to thank his family for their support and patience throughout this study.

1. Summary

Current memories, whether optical or magnetic, are fast approaching their theoretical limits in storage density. This report is an account of the research program undertaken to investigate the potential of spectral holeburning memories for ultra-dense spectral storage. Being atomic scale storage, spectral storage has the potential of providing orders of magnitude denser memories than currently available ones, which depend on the bulk properties of the storage medium. An extensive investigation of novel methods and materials for spectral storage has been carried out. By atomic scale manipulation of the storage medium and applying a novel technique of storage, power-gated holeburning, it has been demonstrated that almost all major barriers to spectral storage can be removed.

A number of rare earth and transition metal doped materials have been studied. In particular, a systematic investigation of alkaline earth sulfides, doped with different rare earth ions, has been carried out as these materials proved to be the most promising class of materials for spectral storage. Of all the systems investigated magnesium and calcium sulfides doped with europium exhibited the most favorable holeburning characteristics. Atomic as well as bulk properties in these materials were optimized to give the best overall performance parameters for a spectral storage device. The most promising characteristics of these materials for ultra-dense storage are:

1. More than a thousand holes can be burned in the optical spectrum of each Eu^{2+} center. In other words, every spatial location as small in size as a focused laser spot, typically a micron square, could store more than a thousand "bits" of information. This is an increase in storage density by three orders of magnitude as compared to current storage densities.
2. Further multiplexing of storage density was possible in thin film multi-layer structures of different sulfides. In this case, every layer consisted of an optical center that stored information in a distinctly different optical center. These centers stored information in different regions of the spectrum. This has the great advantage of addressing such ultra-dense memories in parallel by using as many different lasers as the number of layers.
3. Holeburning is fast, typically completed in nanoseconds. The process of holeburning is resonant two-photon ionization. It is completed in nanoseconds. This is an increase in

speed of writing by six to seven orders of magnitude as compared to the previously established limits for photon-gated persistent holeburning. This makes the speed of writing holeburning memory an order of magnitude faster than current memories.

4. The efficiency of holeburning was exceptionally high due to a prudent choice of rare earth energy levels. The optical transitions involved in holeburning are strongly *electric-dipole allowed*. Their transition strengths approach the theoretical and experimentally observed limits for the strongest transitions in solids.
5. Due to a weak electron-phonon coupling in this system, the loss of optical energy to the phonon bath is also minimal. Therefore heating of the system is reduced during holeburning, which would otherwise create problems of heat dissipation as well as broadening of the spectral holes.
6. The process of holeburning allowed the holes to be cycled to high temperatures, up to 170 K. This would protect the memory against any accidental temperature surges. In addition, it would be possible to at least store memory at relatively high temperatures.
7. Due to the novel mechanism of holeburning, a high density of spectral holes was maintained up to a relatively high temperature, ~ 25 K. This performance is particularly relevant for high temperature operations of holeburning based devices.
8. Finally, the mechanism of holeburning was such that the memory could be erased optically in milliseconds to allow for multiple rewrites.

Research performed and reported here has greatly benefited from a materials research program initiated to atomically tailor and fabricate rare earth doped materials in the form of thin films, two-dimensional multi-layer structures, nano-structures, and nanoparticles. The improvement in the storage characteristics is extremely promising with one exception, the low temperature of operation. Further studies to extend the temperature of operation to higher values would be of immense importance. Another aspect to improve upon is the operational range of spectral holeburning materials. Current materials work in the visible range of the spectrum where the use of bulky dye lasers is a necessity. Operation in the infrared region, where compact solid-state lasers are commercially available, would be an improvement.

2. Personnel Supported

Faculty

1. Dr. Zameer Hasan Principal Investigator, supported for three months summer salary 1996-2001
2. Dr. Edward Gawlinski Supported for one month salary in 1996, one year on project
3. Dr. R Tahir-Kheli Supported for one month salary in 1996, one year on project

Post Doctoral Fellows

1. Dr. Levent Biyikli 1999-2000, Full time
2. Dr. Jihsook Lee Park June 1998, (Part time) September 1998-August 2000 (Full time)
3. Dr. Peter M. Macfarlane December 1996-February 1998, Full time
4. Dr. S.M. Syed Ahmedyan May 1997-June 1998, Part time
5. Dr. Syed Moniruzzaman June 2001- December 2001, Full time
6. Dr. Farit Vagizov Part time

Graduate Students

1. Levent Biyikli Ph.D student, 1996-1999, full time
2. Mikhail Solonenko Ph.D student, 1996-1999, full time
3. Milen Shishkov Ph.D student, 1996 –1999, part time
4. Mohamed Aly Ph.D student, January 1999-December 2001, full time
5. Sameh Dardona Ph.D student, January 2000-December 2001, full time
6. Robert Esposito Ph.D student, 2001 academic year
7. Aras Konjhodzic Ph.D student, 2001 (partly supported)

Doctoral Thesis Completed or in Progress

1. Levent Biyikli - completed 1999, thesis available at the Department of Physics Temple University, Barton Hall 1900 N. 13th Street, Philadelphia, PA 19122
2. Mikhail Solonenko - completed 1999, thesis available at the Department of Physics Temple University, Barton Hall 1900 N. 13th Street, Philadelphia, PA 19122
3. Milen Shishkov - completed 1999, thesis available at the Department of Physics Temple University, Barton Hall 1900 N. 13th Street, Philadelphia, PA 19122
4. Mohamed Aly thesis in progress
5. Sameh Dardona thesis in progress
6. Robert Esposito thesis in progress
7. Aras Konjhodzic thesis in progress

3. Introduction

Conventional storage, whether magnetic or optical, is fast approaching its physical limits. In comparison, spectral storage has the potential of providing orders of magnitude higher densities. The realization of such high-density storage could revolutionize information technology. It would take technology to new frontiers of atomic scale storage where the distinction between the classical and quantum worlds starts disappearing. This is a frontier where new ways of knowing and exploiting matter await great scientific and technological advancements. This report describes the investigations performed on materials and methods of storage in order to explore the possibility of providing a high-density spectral storage medium.

Spectral storage is a special type of optical storage in which information is stored in the optical spectrum of the medium. Therefore, in principle, a single atom can be used to store a bit of information. Hence, a thousand or even a million fold increase in storage densities is possible. Although the possibility of high-density spectral storage using optical holeburning was first discussed more than a quarter-century ago, so far spectral storage has not provided a viable alternative to conventional storage. This is largely due to serious limitations with both the materials and methods of spectral storage.

In the initial stages of these investigations, it was evident that in order to realize a viable device based on spectral storage a multi-dimensional approach was necessary. Therefore, both new materials and novel storage techniques were explored simultaneously during the course of this study. Furthermore, in order to perform these investigations new experimental facilities were required at Temple University. The development of these experimental facilities, although a major task, will not be the subject of this report. This report, therefore, describes two types of research activities undertaken during the course of this grant:

1. Exploring and fabricating new and novel materials.
2. Investigating new and improved techniques for spectral storage.

The technique used for spectral storage described herein was spectral holeburning. If the holes are burned in the optical region of the spectrum the technique is referred to as optical holeburning.

Spectral holes are tiny regions of reduced absorption in the spectrum of the storage medium. Such holes can be created or *burned* by a laser that photo-chemically or photo-

physically alters the optical centers in resonance with its frequency. A laser beam probing the spectrum of the material can read such holes, and therefore, these holes can serve as optical memory. This is shown diagrammatically in Figure 1.

Since the first observation of optical holeburning in solids, almost three decades ago, proposals have been made for its use in high-density memory storage and in communication systems¹⁻³. Progress was hindered by five major factors:

1. A lack of materials in which a high density of spectral holes could be burned.
2. Slow burning processes limiting writing speeds.
3. The erasure of spectral holes (memory) during the reading process.
4. Long-term instability of holes that necessitates a continuous refresh.
5. Cryogenic temperatures of operation to maintain a high density of holes.

An even bigger challenge was to identify a single material that could simultaneously overcome all of the above problems and at the same time compete with the existing memory materials in many more ways.

The work described herein was focused on persistent and gated spectral holeburning materials. In persistent holeburning the spectral holes are permanent and do not deteriorate with time. The gating technique, in addition, prevents deterioration of the hole during readout, which is also carried out by a laser⁴. Otherwise, a continuous refresh of the memory would be necessary.

By atomic scale manipulation of Rare Earths (RE) and other impurities in II-VI hosts, a variety of optical centers were created to serve as storage media. In particular, a systematic investigation of alkaline earth sulfides, doped with different RE ions, was carried out. Of all the systems studied, MgS:Eu exhibited particularly favorable holeburning characteristics. In this material, atomic as well as bulk properties were optimized to give the best overall performance parameters of any persistent holeburning material, such as:

1. Several thousand spectral holes could be burned in one spatial location. This increased the storage density by three orders of magnitude.
2. Fast storage by nanosecond holeburning that increased the storage speed by six to seven orders of magnitude as compared to previous gated materials⁵.

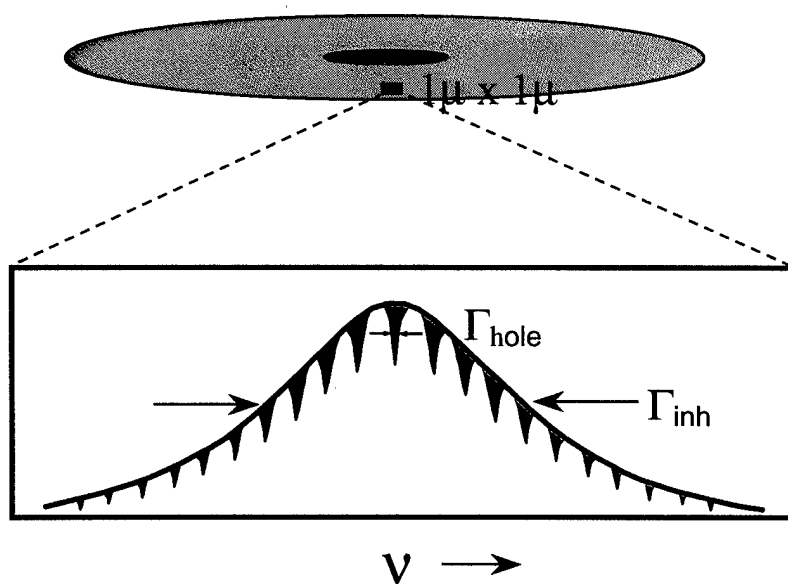


Figure 1: Spectral Storage by Optical Holeburning

3. Extremely high efficiency of holeburning approaching the theoretical limit.
4. Fast optically erasable memory to allow for multiple rewrites.
5. Possible long-term storage of memory at temperatures up to 150 K.
6. Minimization of optical losses by phonons.
7. A high density of spectral holes up to a relatively high temperature, ~ 25 K, an order of magnitude improvement as compared to other materials.

In the following sections a description of the methods of atomically designing and fabricating storage materials and the techniques of spectral holeburning based storage have been described. Detailed results have been presented for the most successful materials. Other materials are only briefly touched on and properly referenced. The prime objective of the investigations was to overcome the limitations of spectral storage. It also remains the common theme of this report. In different sections on methods, results, conclusions, etc., the emphasis is not on making the sections independent but rather self contained and easy to read.

4. Background and Experimental Methods

The focus of this investigation was on materials that exhibit photo-ionization induced photon-gated holeburning. For this type of burning a careful tailoring of the energy levels of the rare earth ion, the band gap of the host material, and the possible valence states of the rare earth ions was necessary. On the other hand, during the course of these investigations a new technique for holeburning, power-gated holeburning, was devised that proved to be very powerful in overcoming the shortcomings of the existing holeburning techniques. The following sections introduce the old and new techniques for holeburning, theoretical background and justification for the materials used, and the experimental setups established to perform high-density spectral holeburning investigations.

4.1 Homogeneous and Inhomogeneous Broadening in Solids

Optical transitions of an impurity ion or molecule in a solid are broadened due to imperfections and impurities present in almost all cases. Such broadening is termed inhomogeneous broadening and can be several orders of magnitude larger than the homogeneous width of these transitions associated with the lifetime uncertainty. Linewidths of optical transitions arising in solids from these two mechanisms, Γ_{inh}, Γ_h , are shown in Figure 2. In optical holeburning a laser selectively addresses and modifies an ensemble of ions/molecules such that they do not absorb at the same frequency as they did prior to this modification. This burns a hole in the absorption spectrum of the material. The width of the hole, Γ_{hole} , depending on the laser can be very narrow and in an ideal case is limited by the homogeneous width, Γ_h . Therefore, a large number of holes, $\Gamma_{inh}/\Gamma_{hole}$, can be burned in an inhomogeneous line profile of a solid. In spectral storage this ratio gives the ideal improvement in density over conventional optical storage. In principle, this ratio can be as high as 10^6 - 10^7 for the transition of a RE ion or an organic molecule in a solid. Recent successful demonstrations of the uses of spectral holeburning in frequency and time domain storage have renewed interest in understanding the physical processes responsible for persistent holeburning so as to develop suitable materials for use in memory and communication applications⁶⁻¹⁰.

In memory applications there were four major areas requiring special attention:

1. The identification of materials with the highest $\Gamma_{inh}/\Gamma_{hole}$ ratio so as to maximize storage density.
2. The stability of spectral holes against the reading beam. If the reading beam can also burn holes it destroys the information in the process of reading it. This problem, common to transient holeburning, can be avoided in photon-gated holeburning, which is inherently persistent^{4,11,12}.
3. The coupling of the electronic states involved in holeburning with lattice spins results in the shifting and broadening of the holes at any temperature, $T > 0$ K. This effect, termed the spectral diffusion of holes, should be eliminated or minimized.
4. A strong coupling of electronic states with the lattice phonons and local vibrations is also undesirable. This causes broadening of the spectral hole and hence the reduction of storage density at non-cryogenic temperatures. This is the most difficult barrier to overcome. Electron-vibration coupling has limited the applications of holeburning, so far, to cryogenic temperatures.

The main challenge has been to identify a single material that could simultaneously overcome all of the above problems. The following sections describe holeburning in RE doped II-VI materials. It is shown that at least in one material all of the above problems, with the exception of the low temperature of operation, could be solved.

4.2 Photon-gated and Power-gated Holeburnings

Photon-gated holeburning (PGHB) was selected as the storage technique because the holes burned by this technique are permanent and at the same time the reading process is nondestructive.

The principle of photon-gated holeburning in its simplest form is shown in Figure 3. It shows the energy levels of the rare earth impurities in a narrow band host. The first photon beam ν_1 selectively excites the optically active ions from their ground state 1 to the excited state 2. Following that, a second beam ν_2 of appropriate energy can further excite these electrons from state 2 to the conduction band where they become delocalized. If Coulomb traps present in the material capture these electrons, a further ionization of the initially excited ions will occur. This will cause a narrow optical hole of width Γ_{hole} , in the absorption spectrum of the ions at energy

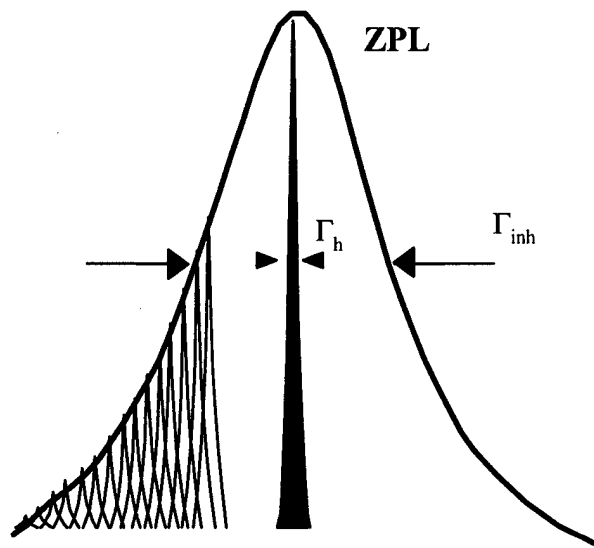


Figure 2. Line Broadening in a solid

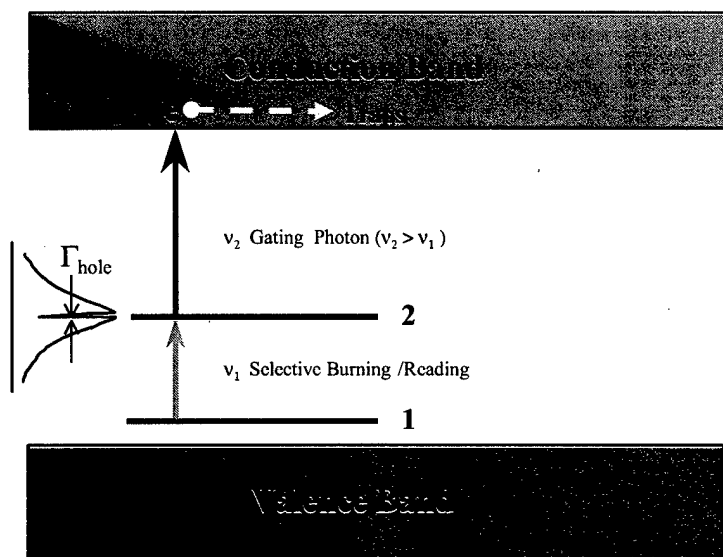


Figure 3. Photon-Gated HoleBurning,

$E = h\nu_1$. The main advantage of gated-holeburning can be seen readily. The hole can be burned only in the presence of two photon beams, ν_1 and ν_2 , while a single photon beam tunable around ν_1 can be used to read it. Such a reading does not cause any writing or erasure.

Power-gated holeburning (POGHB) is a special form of photon-gated holeburning. In this case the two photons have the same frequency, ν , as shown in Figure 4. Holeburning is a *resonant two-photon ionization* process. The frequency selectivity of holeburning results from the presence of one photon resonant transition from state 1 to state 2, for example, in the case of Eu^{2+} in sulfides, the $4f^7-4f^65d^1$ transition. There are several advantages to power-gated holeburning over photon-gated holeburning:

1. A single beam can be used for *burning* as well as *reading* the holes. At high power, where two-photon ionization becomes highly probable the beam can be used for writing or burning the holes, whereas at low powers, where no significant two-photon ionization occurs, it can be used for reading the holes.
2. In photon-gated holeburning a near perfect spatial overlap of the burning and gating beams is needed for writing. Such an overlap creates non-trivial problems, especially for high-density storage devices, where alignment of the beams within a fraction of the wavelength is needed. Using a single beam in power-gated holeburning eliminates this problem.
3. The holeburning process is a two-photon process that is a quadratic function of the intensity of the laser beam. Therefore, the wings of a Gaussian profile, where the intensity is significantly reduced, would not be effective in burning^{13,14}. Hence, the size of the focused laser spot is further reduced for the burning beam. This reduction in size is beyond the diffraction limited focusing, and it would cause an increase in the storage density as well as reduced cross-talks between the bits.
4. And finally, using only one laser in power-gated materials would make the holeburning based devices more compact and economical.

The requirements of efficient and persistent power-gated holeburning impose serious restrictions on the energy levels of the ions involved in holeburning as well as the traps:

1. The energy levels should be placed appropriately in the gap so as to allow power-gated holeburning, i.e., $2h\nu > E_{IC}$, where E_{IC} is the energy separation between the ground state 1 and the conduction band.

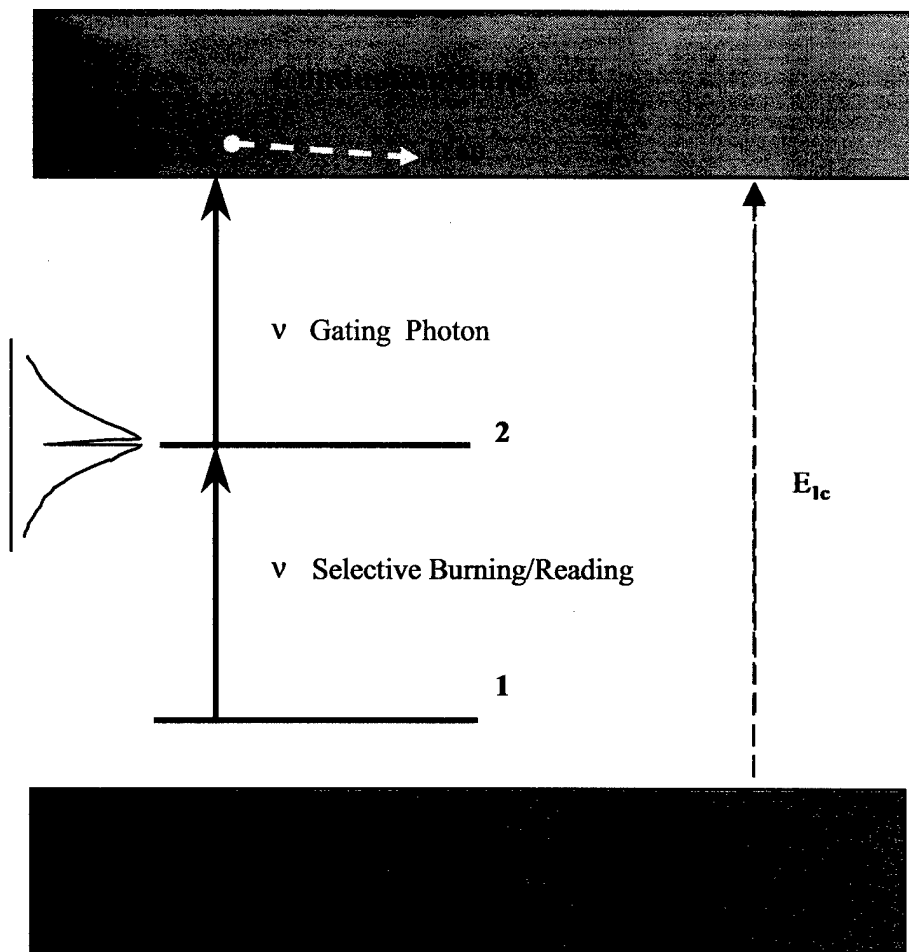


Figure 4. Power-Gated Holeburning, $\nu_1 = \nu_2 = \nu$.

2. For efficient holeburning the oscillator strength, f , of the transition should be as high as possible (the transition at frequency ν in Figure 4).
3. The probability for the non-resonant Two Photon Absorption (TPA), from the ground state to the conduction band, should be as low as possible. Otherwise, during the *writing*, TPA in the conduction band continuum will occur. This would lead to ionization without any frequency selectivity. Hence, the efficiency of writing will be greatly reduced.
4. The energy levels of the traps should be such that there is no significant one- or two-photon absorption by the traps at or around ν , the frequency of reading and writing beams.

4.3 Materials Selection

For photon-gated and power-gated holeburning to be operative it is clear that the medium of storage should have the following characteristics:

1. Strongly allowed transitions of rare earth ions in the visible or near infrared region where tunable lasers can be used for holeburning.
2. A small band gap of the host so that two-photon ionization is possible using the visible and/or the infrared lasers, $E_g \sim 3\text{-}5\text{ eV}$.
3. Two possible stable valence states of the rare earth ion in the host. These ions are used for photo-ionization holeburning as described in the previous section.

As will be described below, rare earth doped II-VI materials satisfy all of these requirements.

4.3.1 Structural Properties

MgS, CaS, SrS and BaS all have the face centered cubic NaCl structure. In MgS, for example, each Mg^{2+} ion is surrounded by six S^{2-} anions and vice versa in forming an octahedron. Both the Eu^{3+} and Eu^{2+} states of Eu are stable in this material. Eu^{2+} substitutes for Mg^{2+} , Figure 5A. However, Eu^{3+} at a substitutional site requires charge compensation that is long range in the present case. The arrows in Figure 5B show the directions of the movements that may be necessary for the charge compensation. The MgS bond is partially covalent with a fractional ionic character of 0.786. The size of Mg^{2+} and S^{2-} ions are 0.66 and 1.84 Å respectively, Table 4.1. The polycrystalline forms of sulfides have high melting temperatures $\sim 2000\text{ }^\circ\text{C}$ ¹⁵. This

presents considerable difficulty in preparing single crystals. In addition, high vapor pressure of the sulfur is necessary to grow these crystals. To date, no single crystal growth of MgS has been reported in literature.

Ion	Atomic Number	Ionic Size (Å)
Mg ²⁺	12	0.660
Ca ²⁺	20	1.0
S ²⁻	16	1.840
Eu ²⁺	63	1.170
Eu ³⁺	63	0.947

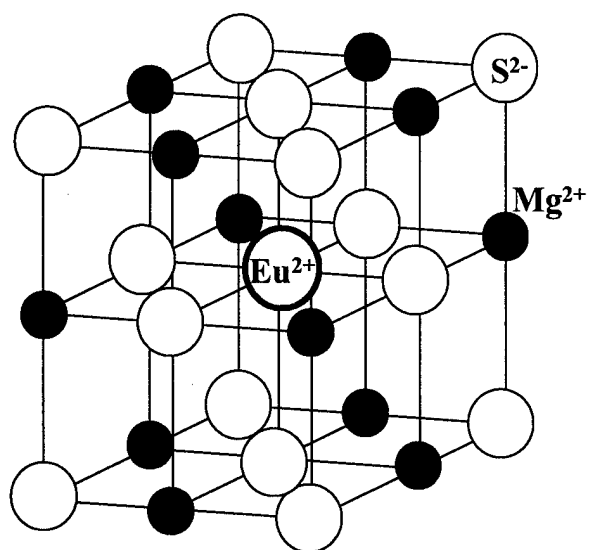
Table 4.1 Table of Ionic Sizes.

4.3.2 Electronic Transitions in Rare Earths for High-Density Storage

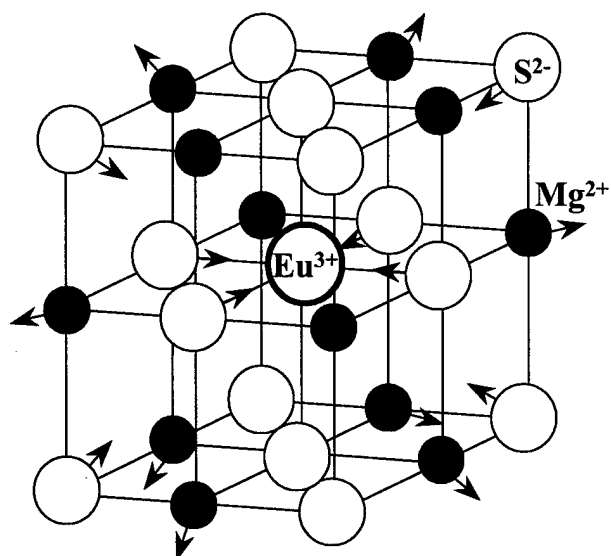
One of the reasons for high-density and efficient holeburning in RE doped II-VI materials is the choice of f-d transitions as opposed to f-f transitions that have been the subject of most of the investigations in the past. Most RE lanthanides, with 4f incomplete shells appear as tripositive ions in inorganic hosts (Ln³⁺). The outer filled 5s and 5p shells shield the 4f electrons of Ln³⁺. Therefore, the crystal field or any other perturbation has a very small effect on their energies. As a result the inhomogeneous broadening of fⁿ levels is generally small, i.e., Γ_{inh} for f-f transitions is small. Even more importantly, optical transitions between these levels are forbidden by electric dipole selection rules ($\Delta l = 0$). Several mixing mechanisms operative in solids weakly allow for these transitions. Therefore, the oscillator strengths for f-f transitions are very weak, ranging from $10^{-6} - 10^{-11}$.

As opposed to f-f, f-d transitions are strongly allowed. d-electrons are also more susceptible to the lattice environment as opposed to f-electrons. This has three important consequences:

1. f-d transitions are strongly electric-dipole allowed, as $\Delta l = 1$ for such transitions. This implies efficient holeburning and a smaller photon budget for reading and writing the memory. For 4f-5d transitions of MgS:Eu, the oscillator strength, $f \sim 0.01$. This should be compared with the f-f transitions, where $f \sim 10^{-6} - 10^{-11}$.



(A)



(B)

Figure 5. Crystal structure of MgS with Eu^{2+} (A) and Eu^{3+} (B)

2. The inhomogeneous broadening of d-levels can be orders of magnitude more than the broadening of f-levels in the same host. This is a great advantage. A broad Γ_{inh} allows for a large number of holes to be burned in a Zero Phonon Line (ZPL).
3. The position of d-levels changes from one host to another appreciably and unpredictably, depending on the strength of the crystal field and other ion-host interactions. This apparent limitation can be an advantage. One of the main objectives of this study was to tailor the energies of ZPL's by changing different host materials and/or RE ions towards the visible-infrared wavelengths. As opposed to f-levels, d-levels allow for such an adjustment in energies.

4.3.3 Theoretical Estimates of 5d- Energy Levels

It is evident that the position of rare earth energy levels with respect to the host band gap is very crucial for gated-holeburning. At the same time, the energies of the holeburning transition should be in the right range of the spectrum where tunable laser sources are available. One obvious question is, "can one calculate and predict the position of 5d-energy levels of a rare earth in II-VI sulfides?" The answer is that it is difficult to calculate energy levels of 5d- electrons in sulfides to any appreciable accuracy. The reason is that the band gaps of these materials are small, and hence, there are not many observed electronic transitions that may be used to extract theoretical parameters to any accuracy. The following calculations for CaS:Eu and MgS:Eu demonstrate this fact.

In order to estimate the energies of the $4f^7-4f^6 5d^1$ transitions of Eu^{2+} in II-VI sulfides the procedure of McClure and Kiss has been followed¹⁶. The results for MgS and CaS are shown in Figure 6. The difference between the free ion energies of $4f^7$ and $4f^6 5d^1$ configurations of Eu^{2+} is $40,430 \text{ cm}^{-1}$. Due to the electrostatic interaction and spin-orbit coupling this energy difference is lowered by 7040 cm^{-1} and 3570 cm^{-1} respectively. Using these rough estimates of electrostatic, H_{es} , and spin-orbit interaction, H_{so} , the energy of $4f^6 5d^1$ state of Eu^{2+} with respect to the free-ion f^n ground state is $29,820 \text{ cm}^{-1}$, Figure 6. In the octahedral crystal field, the $\Gamma_3(e_g)$ state of 5d electron is higher in energy by $6Dq$ than the unsplit $4f^{n-1} 5d^1$ state. The $\Gamma_5(t_{2g})$ level is lowered by $4Dq$ from the unsplit $4f^{n-1} 5d^1$ state. The value of $10Dq$ is estimated from the excitation spectra of CaS:Eu²⁺ and MgS:Eu²⁺, $10Dq = 18570 \text{ cm}^{-1}$ and $19,500 \text{ cm}^{-1}$ respectively. Following this procedure, the energy separation, $4f^7-4f^6 5d^1(t_{2g})$, in CaS and MgS becomes $22,392 \text{ cm}^{-1}$ and

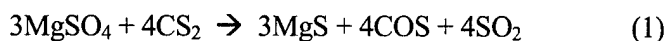
22,020 cm^{-1} respectively¹⁷. However, from the present work, the experimentally determined value of the $4f^7-4f^6 5d^1(t_{2g})$ ZPL in CaS and MgS are $\sim 15,997 \text{ cm}^{-1}$ (625 nm) and $17,301 \text{ cm}^{-1}$ (578 nm) respectively. This disagreement is not surprising for the first order estimate as the validity of this estimation is questionable. One can see from Figure 6 that the contributions of the electrostatic and spin-orbit interactions are smaller than the crystal field splitting of $10Dq$. In such a case, the crystal field should not be included at the last stage of the calculations as a perturbation on the free ion energy levels.

4.4 Material Designing and Processing

For spectral storage it is necessary to engineer the medium at the atomic level. Therefore, materials research was a necessity of this research program. A program for designing and processing these materials was initiated in the earlier stages of the project. As the potential of RE doped II-VI materials for high-density and fast storage became evident, the materials research program grew in its size and capabilities. Rare earth doped sulfides in the form of microparticles, thin films, multi-layer structures, and nanoparticles have been designed and fabricated. The underlying theme was to enhance the spectral storage capabilities. Thin films in multi-layer structures have shown the highest density of storage by gated-holeburning.

4.4.1 Microparticles of RE-Doped II-VI Sulfides

The samples of sulfides doped with rare earths were prepared in our crystal growth laboratory. The schematic of the setup is shown in Figure 7. Starting materials were of high purity, 99.99% or higher. For MgS:RE samples the starting materials were $\text{MgSO}_4 \cdot 7\text{H}_2\text{O}$ and a small fraction of oxides of the respective RE. The commercially available magnesium sulfate contains seven molecules of water per MgSO_4 molecule. The first step in preparing the samples was to completely remove this water by heating. The powder sample of $\text{MgSO}_4 \cdot 7\text{H}_2\text{O}$ was placed in a box furnace at 950°C for a duration of 12 to 16 hours. In the second step MgS was obtained by the reduction of MgSO_4 through a heat treatment in a reducing atmosphere of CS_2 . The chemical reaction process is as follows¹⁸:



The samples thus obtained were high quality white powders with particle sizes ranging from a few microns to tens of microns. The final step in this process was to dope the MgS with

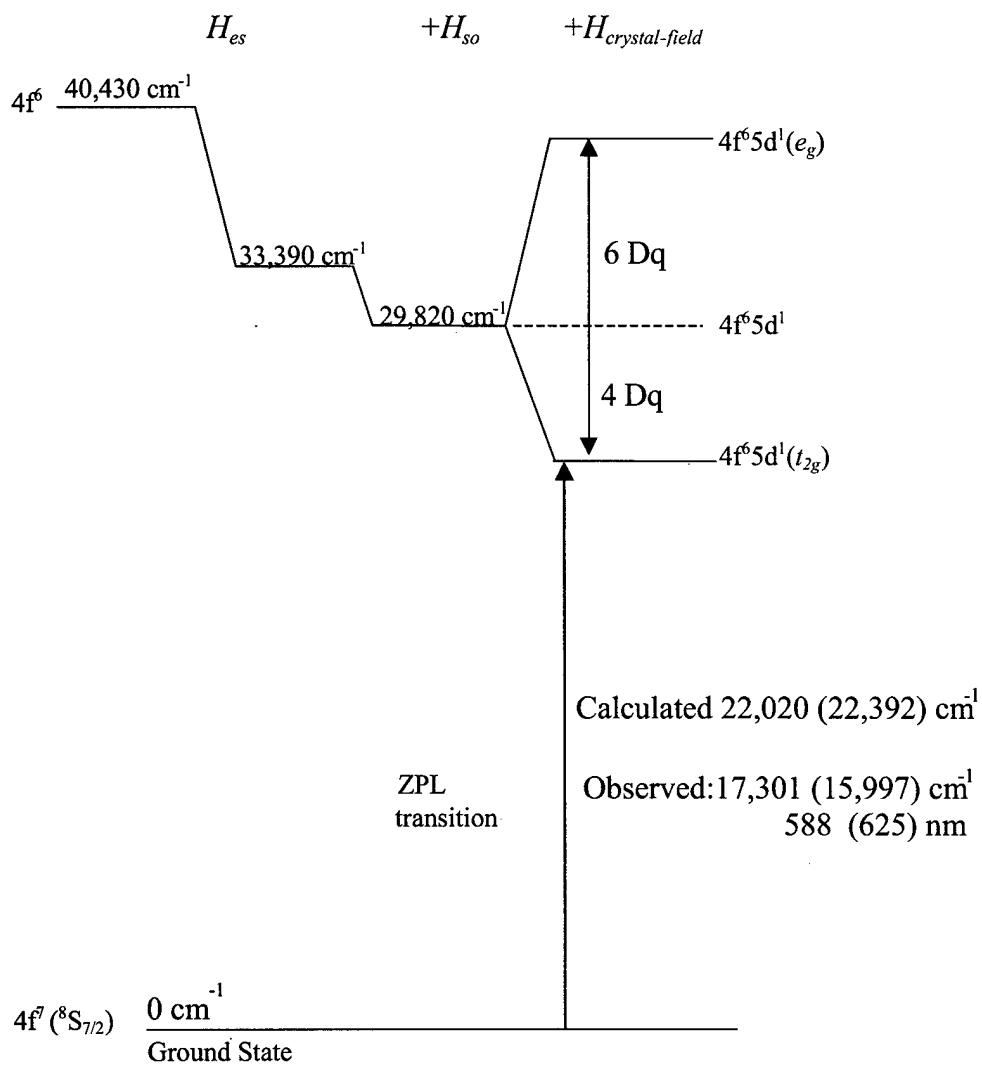


Figure 6. First order estimates of the relevant Eu^{2+} energy levels in MgS and CaS . Calculated and experimentally observed values for CaS are given in parentheses. $Dq = 1950$ (and 1857 cm^{-1} for CaS)

the appropriate rare earth. This was achieved by diffusion of rare earth ions at elevated temperatures. Appropriate amounts of MgS and rare earth oxides were thoroughly ground and mixed together in the open atmosphere at room temperature. The mixture was placed in a silica crucible inside a quartz tube where it was heat treated at 950 °C for a few hours to diffuse the rare earth material. The reducing atmosphere, as in the previous step, was maintained by passing a stream of Argon gas carrying traces of CS₂. The sample was subsequently cooled down to room temperature while the flow of CS₂ carrying buffer argon gas was continued. The resulting samples were light yellow to orange in appearance depending on the concentration of Eu in them. The particle sizes of the powder were generally in the range of 1 to 10 microns.

Parameters such as the flow rate of the gas, temperature, and time of treatment for the reduction and the diffusion of rare earth were optimized. This was done to incorporate the right rare earth ion with the optimum concentration at the desired lattice sites in the crystal. This was realized by maximizing the characteristic emission of the desired rare earth sites from the sample.

4.4.2 Thin Film and Multi-Layer Structures

Single crystals of RE doped sulfides are very difficult to grow due to their high melting points and the controlled chemical environment required during growth. In any case, single crystals would accommodate Eu predominantly in the divalent state. Hence, they would not allow for the large concentration of Eu³⁺ traps needed for efficient photon-gated holeburning¹⁹. Laser Pulsed Vapor Deposition (LPVD) under controlled chemical conditions was developed in-house to prepare thin film and multi-layer structures. These films exhibit the highest density of storage by the gated holeburning technique. The pulsed laser deposition system is shown in Figure 8. Its special features include:

1. Multiple targets: up to four different targets can be loaded on a rotating mount, allowing thin films of four different materials to be deposited simultaneously.
2. The chemical environment in the chamber can be controlled. This allows for pure RE as well as impurity associated RE optical centers to be engineered in the material. New impurity-associated centers essentially increase the number of potential ZPL's available for holeburning and hence storage density.
3. The substrate holder assembly of this system can also hold four substrates on a rotating mount. Therefore, in one run four samples can be prepared.

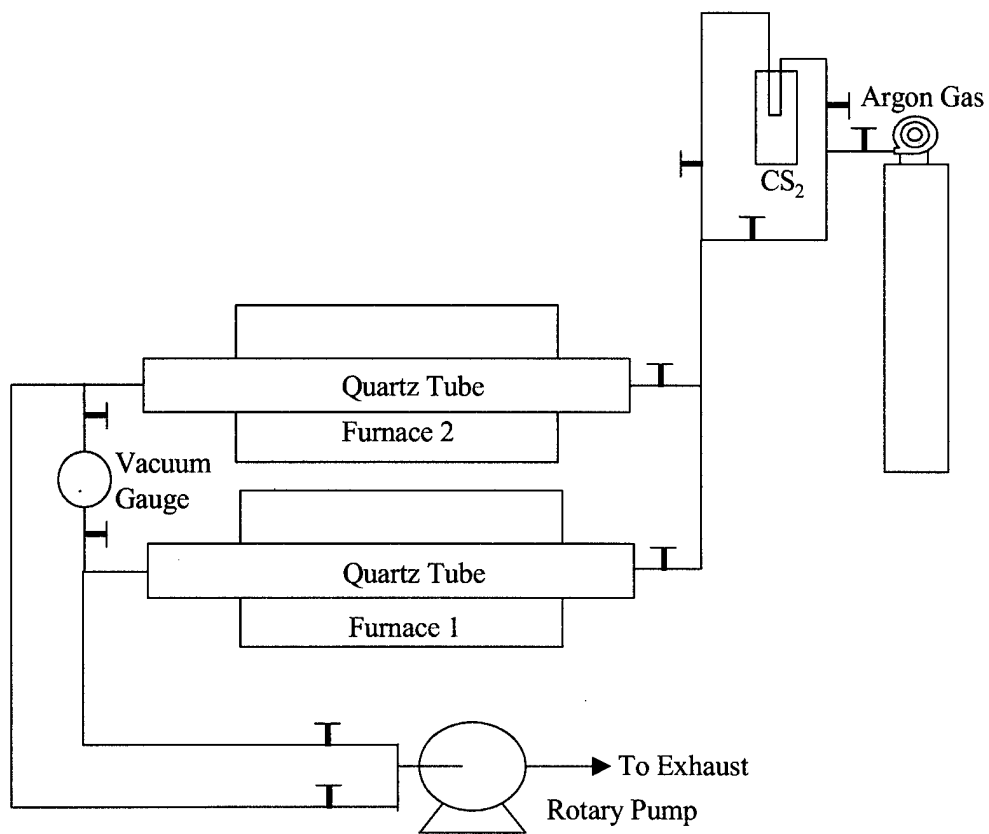


Figure 7. Experimental setup for the microparticles.

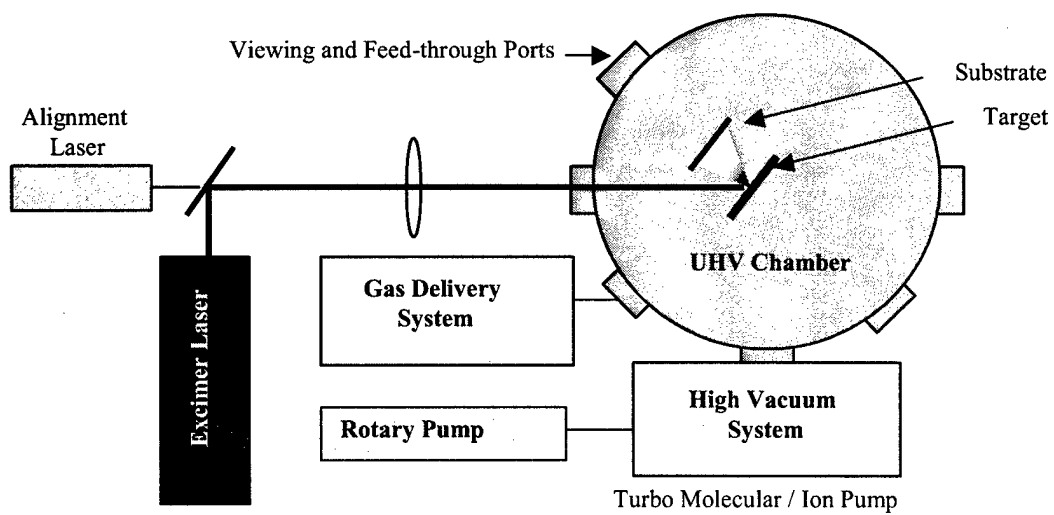


Figure 8. LPVD Setup for Thin Film Deposition

It has been found that in CaS:Eu and MgS:Eu high concentrations of Eu^{3+} , as much as 10 times the concentration of Eu^{2+} , can be produced in microparticles. Obviously, such microparticles demonstrated very efficient holeburning. When starting materials for targets with such high Eu^{3+} concentration are used, changing the chemical environment of growth can control the concentration of Eu^{2+} . Using the LPVD technique, thin films have been prepared that have holeburning properties as favorable as those of microparticles²⁰.

Solid pallets of the desired RE doped II-VI material served as the targets that were ablated by a high power pulsed excimer laser. These pallets were formed by compacting microparticles and were also prepared in-house. Laser ablated vapors were deposited on a single crystal MgO substrate to form thin films. The main advantage of this setup is its flexibility. Introducing different gases in the chamber can control the chemical environment during the growth. Changing the atmosphere of growth of the films can alter the relative concentration of RE^{2+} and RE^{3+} in the sample. A complete investigation of growth characteristics by varying different parameter was undertaken.

Major advantages of holeburning in thin films are as follows:

1. Thin films have been grown where holes can be burned with the same high density as that for the microparticles (1000 or more holes per ZPL).
2. Thin films are glassy in nature as opposed to the microparticles that are polycrystalline. Therefore, the inhomogeneous width of the ZPL, Γ_{inh} , and hence the number of holes, can be controlled by the growth conditions. This is a unique advantage with the films.
3. The thickness of films can be varied for three-dimensional samples.
4. Finally, and even more importantly, multi-layer structures of different materials can be grown to store information with spatial and spectral selectivity. This is described below.

4.4.3 Multi-Layer Thin Film Fabrication (LPVD)

The concept of multiplexing information storage in multi-layer structures has also been experimentally demonstrated. In this case each layer is made up of a different atomically engineered material²¹. This is possible by either changing the chemical conditions of growth or the target material in LPVD chamber, or both. ZPL's in these materials lie at different energies. For example, ZPL's of 4f-5d transitions of Eu^{2+} in MgS, CaS, and oxygenated MgS lie at 575,

625 and 589 nm, respectively. All three centers show efficient holeburning and have been deposited in layers over each other, using the experimental set-up of Figure 8. Figure 9, shows schematically the parallel optical addressing possible with different color beams in such structures.

4.4.4 Nanoparticles by Quench Condensation of Laser Ablated Vapors

Having small size and a large surface to volume ratio, nanoparticles are expected to show more efficient holeburning and distinctly different electron-phonon coupling properties than that of the bulk material. The setup for the production of nanoparticles is schematically shown in Figure 10. The nanoparticles are prepared as follows:

1. A pallet of RE doped II-VI material is ablated by a high power pulsed excimer laser.
2. These vapors are quench-condensed on a gold substrate maintained at 77K by thermal contact with a liquid nitrogen reservoir.
3. Introducing an inert buffer gas in the chamber and varying its pressure gives control on the size of nanoparticles.
4. Changing the ambient gas can control relative concentration of RE^{2+} and RE^{3+} in nanoparticles²².

4.5 Material Characterization

The characterization of materials is an essential part of developing new materials. For atomically engineered optical materials particularly, there were two types of characterizations: one for the bulk properties and the other for the quantum properties of specific optical centers that are to be used for holeburning and other photonic applications. The latter involves detailed laser spectroscopic investigations and is covered separately in the following section.

Physical and chemical properties of materials were characterized using conventional techniques such as X-rays, optical microscopy, and electron microscopies including Transmission Electron Microscopy (TEM) and Scanning Electron Microscopy (SEM).

X-ray diffraction was used to determine the crystalline nature of samples. In the case of sulfides, microparticles samples were found to be polycrystalline, whereas nanoparticles and thin films were generally glassy in nature.

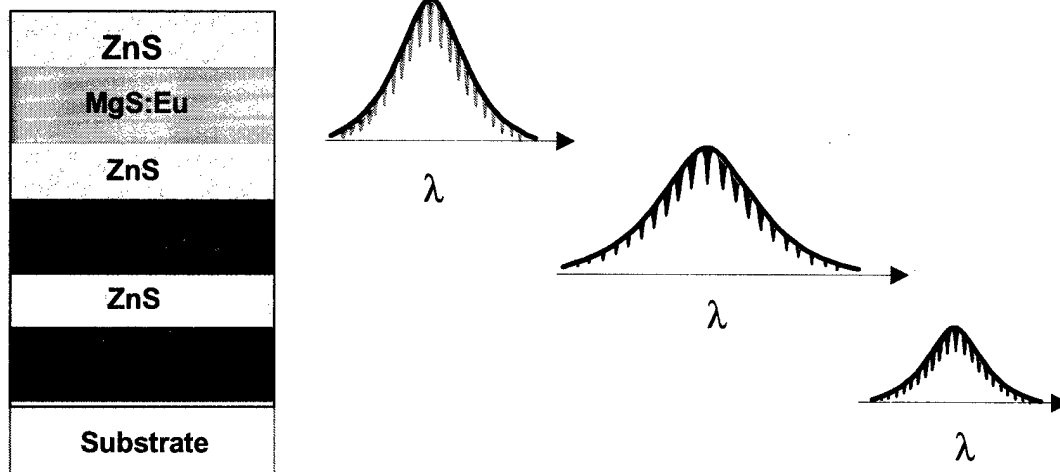


Figure 9. Schematics of Parallel Optical Storage and addressing in Multi-Center-Multi-Layer Structures

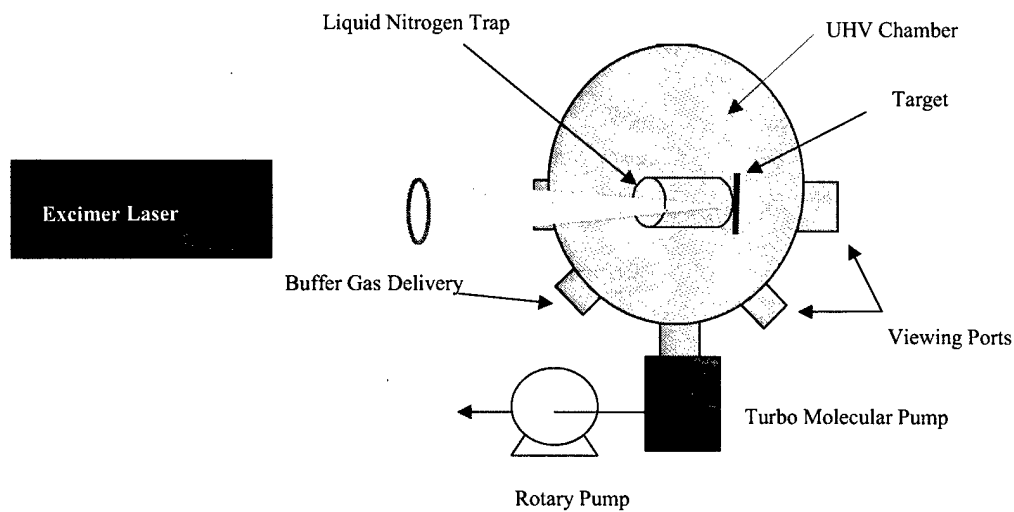


Figure 10. Nanoparticle Production Setup

Optical microscopy provided information on the homogeneity of growth and an estimate of the concentration of scattering centers in the thin film samples. Surface profilometry was performed on the thin film structures to quantify their thickness and uniformity. For microparticles optical microscopy provided useful information on the size and crystalline faces of the polycrystalline material.

The facilities of the Material Research Laboratory of the University of Pennsylvania were used for electron microscopy.

4.5.1 Mössbauer Studies of $\text{Eu}^{2+}/\text{Eu}^{3+}$ Based Materials

In case of Eu-based materials, holeburning requires the presence of both Eu^{2+} and Eu^{3+} centers. In principle, for samples containing Eu, Mössbauer experiments can provide information on the ratio of Eu^{3+} and Eu^{2+} concentrations. Some of these experiments were performed as a part of an ONR/AFOSR funded project on Mössbauer optical double resonance. Mössbauer measurements for low concentrations of Eu ~ 0.01 mol % were especially challenging and required very long data accumulation times.

4.5.2 Optical Characterization

Typical concentrations of rare earth impurities in our samples were ~ 0.01 mol %. Optical characterization is the only way to determine the presence of the appropriate rare earth centers in the sample. The types of optical measurements performed on the sample were absorption studies, using Cary 519, and emission studies on an optical system built in-house. Low temperature emission was found to be the most powerful technique in determining the presence of the desired RE optical-center. Absorption from scattering samples such a polycrystalline microparticles was studied by using special optical accessories that collect and detect scattered optical signals in a large solid angle. Several such accessories were available for our experimental setup.

4.6 Experimental Procedures for Optical Studies

Commercially available instruments were used only for low-resolution absorption experiments that were essential for material characterization. For all other optical investigations,

particularly at high-energy resolutions, experimental setups were designed in-house using commercially available components such as lasers, detectors, and optical accessories.

4.6.1 Absorption, Emission and Excitation Setups

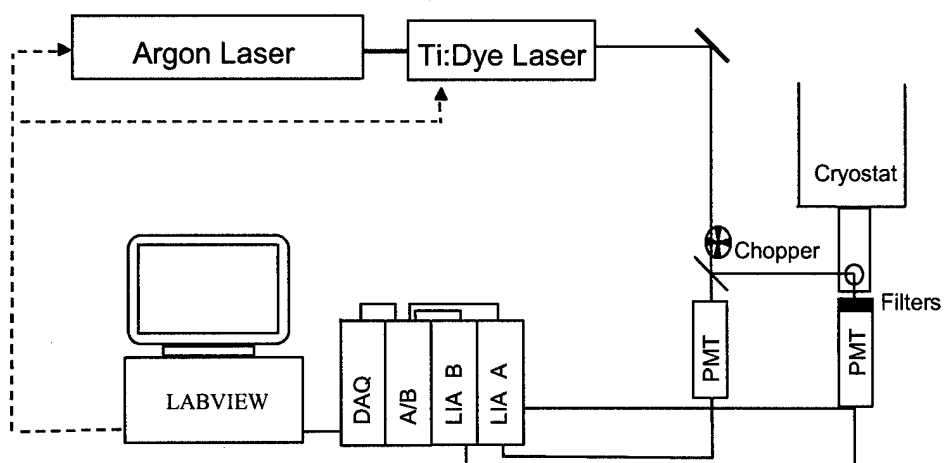
Cary 219 and 519 Spectrophotometers: These instruments were used for low-resolution absorption spectra. Together these instruments cover a spectral range from 100 to 1000 nm. The instruments were controlled externally by using a personal computer. The samples mounted on a cold finger of a closed cycle refrigerator could be inserted into the sample space. In this manner, these instruments allowed for the recording of absorption as well as the transmission spectra of the sample in the temperature range from 10 to 300 K. The resolution of the Cary 219 and 519 instruments was better than ± 0.1 nm.

Excitation and Emission Setup: For better resolutions in shorter spectral range a dye laser based setup was used, Figure 11A. In the excitation mode, its resolution is limited by the resolution of the laser, 0.03 cm^{-1} . In the emission mode, the resolution is limited by the resolution of the monochromator, 0.1 cm^{-1} . For the recording of the excitation spectra, the tunable laser beam was directed to the sample. The scattered laser light was filtered out and only the emission from the sample was focused onto a photomultiplier tube. In order to improve the signal to noise ratio, a phase sensitive detection using a light chopper and a lock-in amplifier was employed. The signal was normalized to the fluctuations in the laser power. The incident laser beam was split into two, the reference and the sample beams. The signal from the photomultiplier tube was divided by the power of the reference beam.

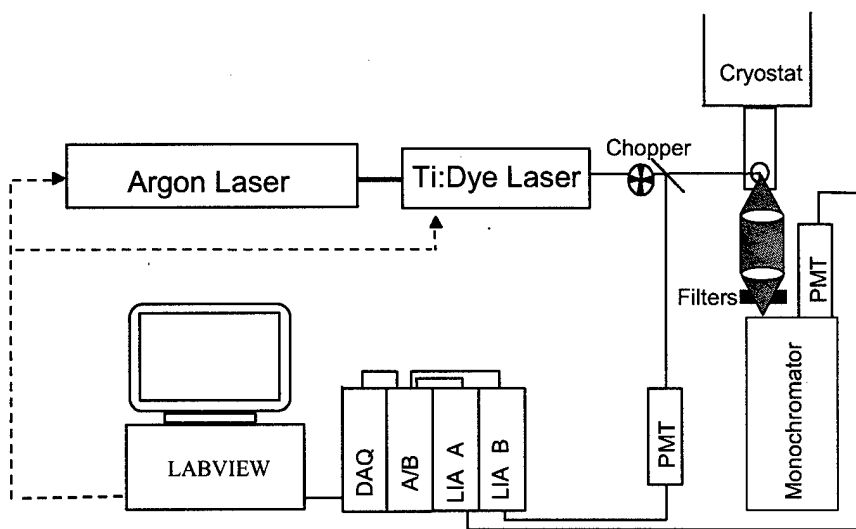
For the emission mode, the laser was fixed to the desired excitation wavelength and focused on the sample, Figure 11B. The emission from the sample was focused onto the slit of the Spex 750 M monochromator. Appropriate filters were used to block the scattered laser light. The emission spectra were obtained by scanning the monochromator over the desired range.

4.6.2 Pulsed Setup

This setup, Figure 12, was used for lifetime measurements and in slightly modified form for fast, nanosecond holeburning experiments. A Lambda Physik excimer laser Compex 102 was used for pumping the Lambda Physik LPD 3000 dye laser system. The output of the



(A) Excitation setup.



(B) Emission setup.

Figure 11. The Excitation and emission setup.

excimer laser was in the form of 10 ns laser pulses with a maximum repetition rate of 100 Hz. The laser used a Xenon-Chlorine mixture that lases at 308 nm. It produces a maximum pulse energy of 200 mJ. This laser was controlled through trigger pulses from the dye laser. Each of these trigger pulses resulted in a laser pulse within 500 ns of the trigger. The dye laser had a GBIP interface and was controlled by computer through the software developed in LabView. By using the GBIP interface, the computer also controlled the trigger pulses that were generated from the dye laser. The detection system for lifetime measurements consisted of a photomultiplier tube (PMT), a boxcar integrator, and a preamplifier. The setup was completely synchronized by the trigger pulses generated from the dye laser, as shown in Figure 13. The laser beam was focused onto the sample. The emission was collected through a lens assembly and focused on the slit of Spex 750M monochromator at 90 degree with respect to the laser beam, Figure 12.

For the detection of the emission signal a Thorn EMI 9816B gated PMT was used. The PMT could be turned on and off by a gating circuit. The gated PMT was turned off during the laser pulse to prevent PMT overload due to the scattered laser radiation reaching it. This gating circuit changes the potential of the first dynode to be positive or negative with respect to cathode. In this manner electrons from the cathode surface are repelled during the off time and amplified during the on time.

The gating circuit had a limitation of 2 μ s transition time between the on and off mode. The signal was amplified and recorded by a boxcar integrator. The gate delay and width for the boxcar integrator was varied as required for measuring the emission from the sample. For lifetime measurements, the gate was scanned over a time range of interest. In this manner emission from the sample was monitored following the sharp laser pulse.

4.6.3 High-Resolution Optical Holeburning Setup

This setup as shown in Figure 14A, was used for photon-gated and power-gated holeburning experiments. The heart of this setup is a Coherent 899-29 Ti-Dye laser that was employed for burning, erasing, and reading the spectral holes. A Coherent Sabre DBW 25/5 Ar-ion Laser was used to pump the Ti-dye laser system. It had a maximum output power of 30 watts in the multi-line visible mode (456 to 528 nm range) and 5 watts in the multi-line UV mode (300 to 400 nm

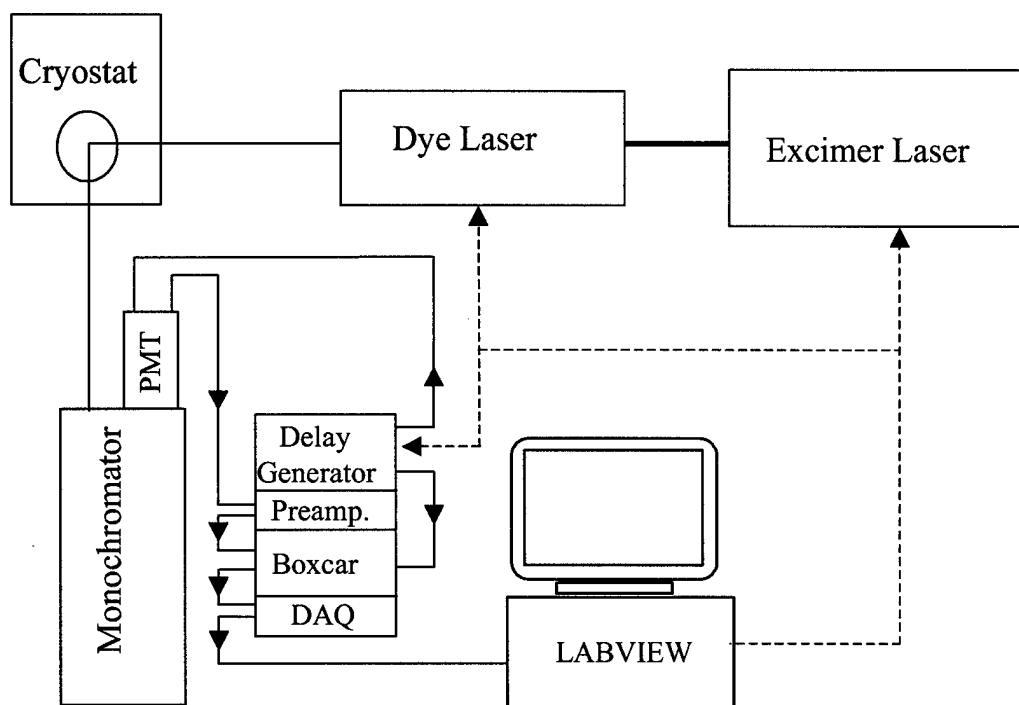


Figure 12. Experimental setup for lifetime, pulsed fluorescence excitation and emission measurements

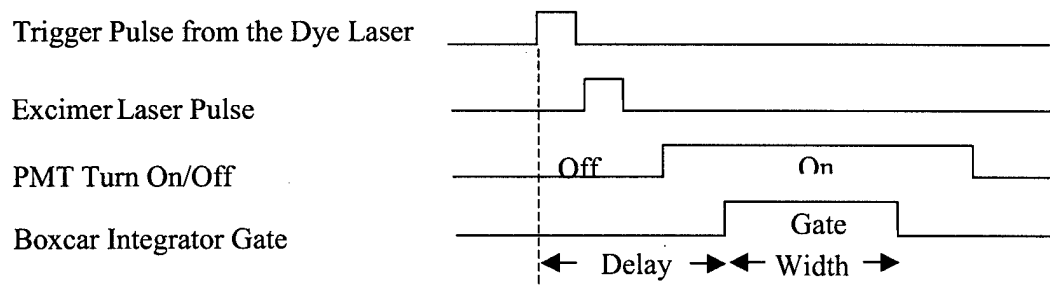


Figure 13. Synchronization of the pulsed setup.

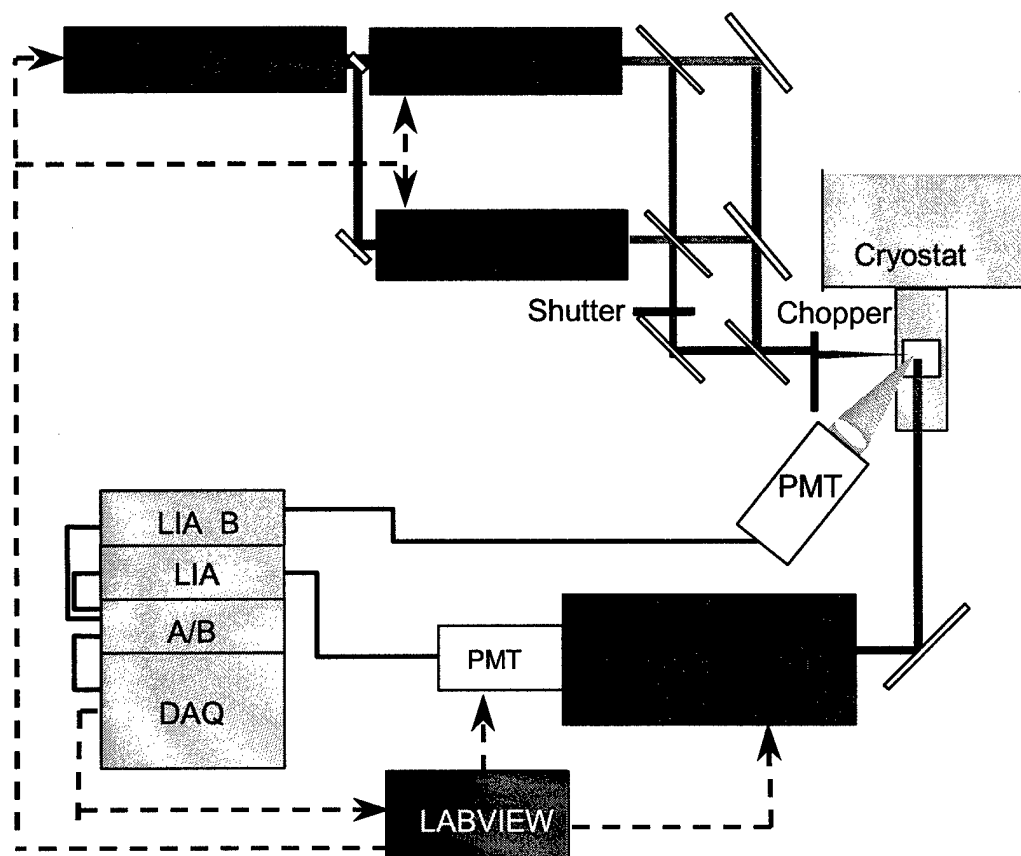


Figure 14A. Experimental set up for cw photon-gated and power-gated holeburning.

range). The same laser was also used as a source of excitation for some of the emission measurements.

The Coherent 899-29 laser system is a convertible laser system that can operate as a conventional ring dye laser or as a solid state ring laser by using Ti-sapphire as the gain medium. It is tunable from 375 to 890 nm in dye operations and from 680 to 1025 nm as a solid state ring laser in Ti-sapphire mode. The system consists of a Ti/dye laser, a control box with a computer interface box and a wavelength meter. To scan more than 30 GHz (1 cm^{-1}), it is necessary to use the autoscan option of the laser. Autoscan uses the wavemeter and synchronously controls different optical components of the laser such as the etalon and Brewster plates to scan over a large range in 10 GHz segments.

The beam from the dye laser is split into two beams. One of the beams is of low intensity. It was used for reading the spectral holes, or the emission and excitation spectra. The other beam is higher in intensity. It was used for burning the spectral holes. These two beams followed the same optical path leading to the sample. The read beam was modulated by a mechanical chopper. A phase sensitive detection was used employing lock-in amplifiers (Ithaco model # 593, Stanford research model # SR 830 and SR 530). The signal was normalized to the fluctuations in the laser power by using a reference channel. A Stanford research analog processor model # SR 235 was used to divide the monitored signal by the reference channel signal in real time. The write (holeburning) beam was computer controlled through a mechanical electromagnetic shutter. An interface box was designed such that TTL pulses from the computer turned the shutter on or off. Using this system the 'on time' could be set to a value as low as 5 ms. The on-time was used to burn the holes.

For nanosecond holeburning, the excimer pumped pulsed dye laser was used, but the present cw setup was used to read holes, Figure 14B. As all holeburning experiments required scanning in THz range, the laser was controlled by an external computer using Labview software.

4.7 Cryogenics

Most of the spectral holeburning experiments were performed at or around liquid helium temperatures, 4.2 K. For other experiments the temperature of the samples was varied from 1.5 to 300 K.

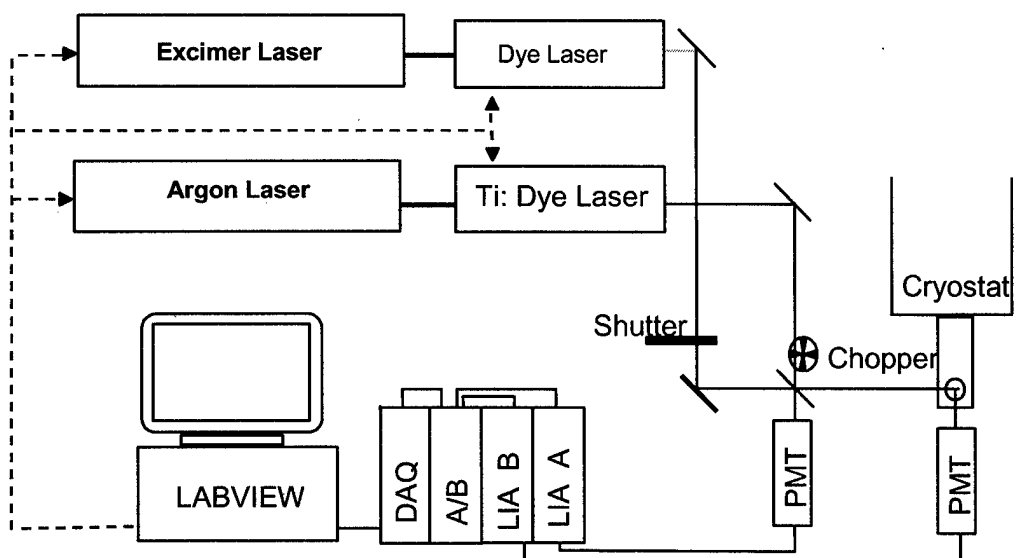


Figure 14B. Experimental setup for nanosecond holeburning.

For excitation and emission measurements the sample temperature was typically varied from 7 to 300 K. This was possible by using an APD Industries, Displex DE-202 closed cycle refrigerator. The samples were mounted on a copper holder attached to the cold finger of the closed cycle refrigerator. To provide good thermal conduction an indium seal was placed in between the contacts.

For temperatures at or below liquid helium temperature, down to 1.3 K, a Cryo Industries liquid helium immersion cryostat, model CIOCC-200-2-R was used. Sample temperature in this cryostat could be varied from 1.3 to 350 K. The stabilization in temperature was achieved by a resistive heater element situated next to the sample. The heater element was controlled by a temperature controller, Scientific Instruments model 9620. The temperature controller provided a stable temperature to ± 0.5 K of the actual temperature with an accuracy of ± 0.2 K. The temperature of the sample was monitored using a silicon diode that had an accuracy of ± 0.5 K for the temperature range 0 to 100 K and ± 1 % of the measured value in the 100 to 475 K range.

5. Results and Discussion

Ultra-high-density and fast storage has been demonstrated in RE doped sulfides using the novel technique of power-gated holeburning. A careful tailoring of the host energy band structure and the RE energy levels involved in holeburning and an optimization of the concentration of deep electron traps allowed POGHB to be fast and efficient. In the subsequent sections it has been shown that such atomically tailored materials not only exhibit fast storage with the highest possible density, but also have the most promising other characteristics for a persistent spectral storage medium.

Many combinations of hosts (CaS, MgS, SrS, etc.) and RE ions (Eu, Nd, Ce, Pr, Tb, etc.) were investigated. The most successful among these materials was MgS:Eu. This material exhibited: the highest density of gated holes in a Zero Phonon Line (ZPL); the fastest reported speed for gated-burning; the highest efficiency for gated-holeburning; high temperature cycling up to 150 K and; complete photo-erasability. During the course of our investigations it became clear that this material should be optimized for all properties relevant to a practical memory device. Therefore, materials based on MgS:Eu were developed to overcome the practical limitations of a viable device. In the following, the favorable features of holeburning in rare earth doped II-VI materials, taking an example of MgS:Eu, are described. For the sake of brevity, results on other systems, with different combinations of RE and II-VI host, will only be summarized and the reader would be referred to appropriate published material.

5.1 Ultra-High-Density Storage in MgS:Eu

Figure 15 shows the ZPL of MgS:Eu²⁺, at $\lambda = 578$ nm, the shaded area. Two hundred and forty holes were burned in the $4f^7-4f^65d^1$ transition of Eu²⁺, as shown in the lower part of the figure. These holes were burned with 25 mW/cm² of cw laser power incident for 2 seconds on microparticle samples that were cooled down to a temperature of 2.1 K.

As the inhomogeneous broadening of d-levels can be orders of magnitude larger than the broadening of f-levels in the same host, a broad Γ_{inh} allows for a large number of holes to be burned in a ZPL. In the present case the entire 2 THz region can be used for burning holes. Typical holewidth, Γ_{hole} , was around 5 GHz, although the narrowest holewidth was $\Gamma_{hole}=1.2\text{GHz}$, $\Gamma_{inh}/\Gamma_{hole} \sim 2000$. Therefore, in principle, more than a thousand holes can be burned in this ZPL.

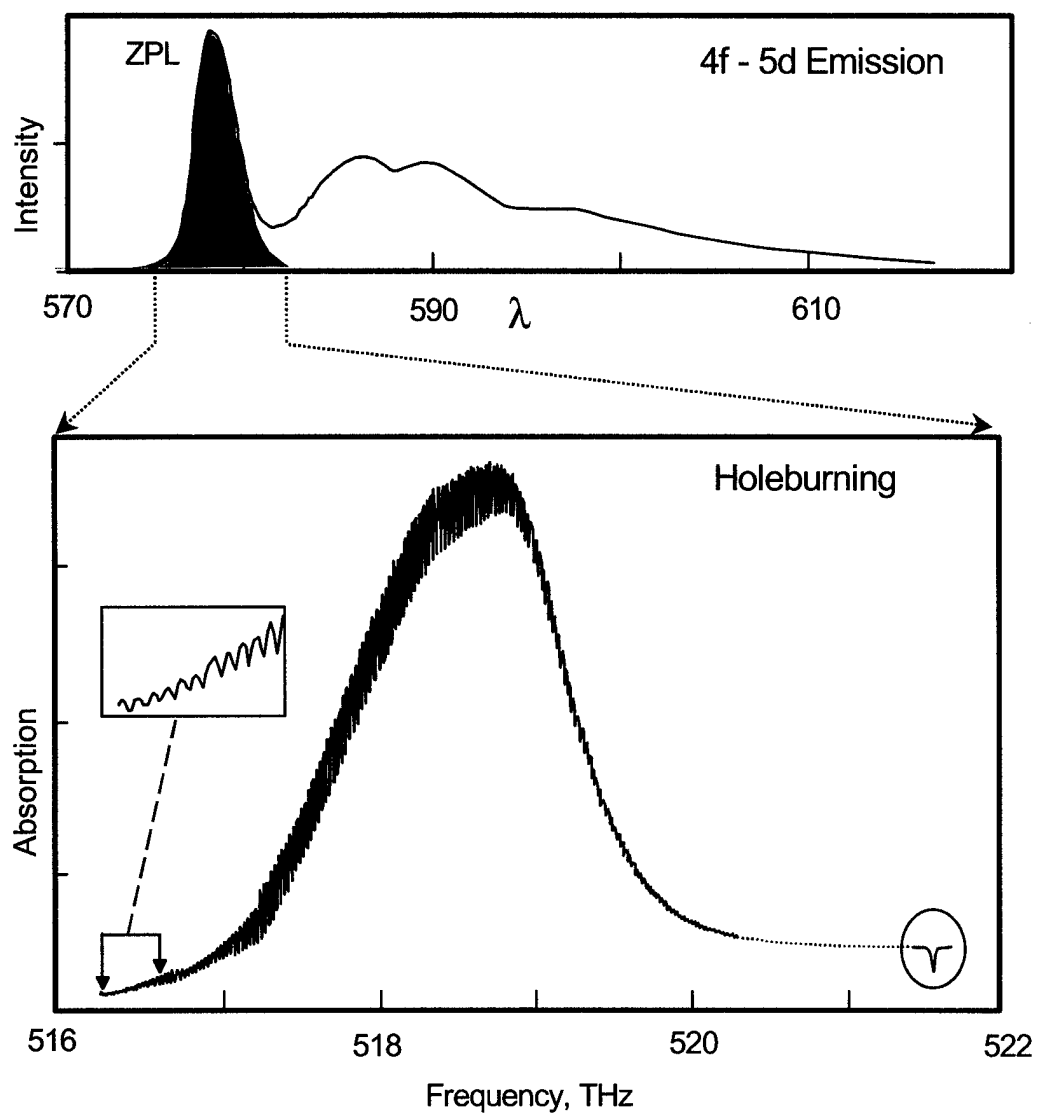
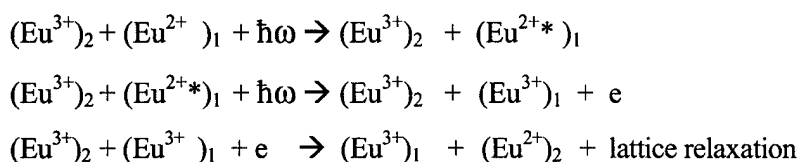


Figure 15. Several hundred holes burned in MgS:Eu

f-d transitions are strongly electric-dipole allowed, hence the holes can be burned far away in the wings, as shown in Figure 15.

5.1.1 Mechanism of Holeburning

The holeburning process in MgS:Eu microparticles is power-gated photo-ionization holeburning, as the two-step photo-ionization of Eu^{2+} is responsible for the burning. The holeburning process is described by the following equations:



where $\hbar\omega$ represents both the burning and the gating photons. The asterisk indicates that the ion is in the excited state.

This holeburning mechanism creates one new Eu^{2+} for every one ionized. The local environment of this new Eu^{2+} will in general be different from the one ionized. Therefore, the ZPL of this new Eu^{2+} can be anywhere in the inhomogeneously broadened profile. Some important features of the above holeburning process in MgS are²³⁻²⁵:

1. A detailed balance between the number of Eu^{3+} and Eu^{2+} ions is maintained. Since Eu^{2+} and Eu^{3+} are both energetically stable, the system after holeburning is overall as stable as it was prior to it. Therefore, holeburning is permanent. Ideally, the holes can last forever at low temperatures.
2. Holeburning is very efficient. Both the 4f-5d and 5d-conduction band transitions are electric dipole allowed transitions.
3. There is an adequate density of Eu^{3+} traps to allow for up to 100% deep burning of the holes.
4. Burning a hole in one part of the inhomogeneous line does not create a sharp side hole or antihole in another location. Therefore, the entire inhomogeneous line is available for holeburning, giving rise to very high-density storage.

This holeburning mechanism implies that hole formation is accompanied by an increase in signal from the other parts of the inhomogeneous profile. In other words, the second hole burned partly fills the first hole that was burned at the same spatial location in the sample. This may appear to be a disadvantage. However, if the number of ions involved in the holeburning process is much smaller than the total number of ions, a slight erasure caused by burning additional holes is not a limitation on the maximum number of holes that can be burned in the ZPL.

In MgS:Eu^{2+} very little power is needed to read the holes because of the very strongly allowed $4f^n - 4f^{n-1} 5d^1$ transition. In power-gated holeburning, reading is a one-photon process. On the other hand, burning is a two-photon process, and it depends quadratically on the power of the laser. In these experiments the reading beam power was four orders of magnitude less than the burning beam power. Because of the low power level of the reading beam, there is almost no burning. At high power levels burning can be achieved in short durations of time (in 10 ns in pulsed and 5 ms in cw setup).

5.1.2 High Efficiency of Holeburning

The mechanism of holeburning in MgS:Eu is highly efficient. This high efficiency is due to mainly three reasons:

1. The $4f-5d$ transition involved in holeburning is highly allowed with oscillator strength $f \sim 0.01$ as discussed above. This makes reading and writing more efficient.
2. The concentration of Eu^{3+} ions that acts as deep traps during the holeburning process has been optimized. As a result, the electrons released to the conduction band are very efficiently captured. This results in very efficient photo-ionization and hence holeburning. A concentration ratio of Eu^{2+} to Eu^{3+} of 1:10 has been produced in the samples for enhancing the capture cross-section.
3. The energy levels and the selection rules for the optical transitions are such that the losses due to the absorption in the phonon side bands of Eu^{2+} and the absorption by traps have been minimized; thus the quantum efficiency of holeburning has been maximized. The Debye-Waller Factor (DWF) for the ZPL's used in holeburning is

very close to the ideal value of unity ($DWF \geq 0.95$). Therefore, almost 100% deep holes can be burned in $MgS:Eu^{2+}$ ^(26,27).

4. Holeburning in $CaS:Eu$ is not as efficient as in $MgS:Eu$. With $CaS:Eu$, the DWF factor is much smaller in comparison, of the order of 0.3, and the selection rules for the 4f-5d electronic transitions are not as favorable as in the case of $MgS:Eu$.

5.1.3 Fast Writing

Typical burning times of photon-gated holeburning materials have been in the seconds to hundreds of a second time range²⁸. Both $CaS:Eu$ and $MgS:Eu$ show the fastest burning times of any gated-holeburning material. Not only are holeburning times fast, but the speed of burning exceeds the limit set for magnetic memories, the fastest memories available to date.

Fast burning of holes in these materials is mainly due to three reasons:

1. The holeburning process is a resonant two-photon ionization of Eu^{2+} . This process is inherently fast and is completed in the nanosecond timescale.
2. At high concentrations, Eu^{3+} traps efficiently capture the released electrons and cause ionization with a high duty cycle. Therefore, multiple excitation cycles are not needed for a detectable hole. Figure 16A shows the holes burned by 10 nanosecond pulses.
3. The power gated holeburning in $CaS:Eu$ is as fast as in $MgS:Eu$. However, the efficiency of burning is considerably less.

It should be noted that this speed of burning is limited by the width of the laser pulse used. In principle, the speed of holeburning can be further increased by at least two orders of magnitude before the Fourier transform limit of the short pulse ($\Delta\tau = 0.1$ ns, $\Delta\nu = 1.6$ GHz) starts exceeding the holewidth, $\Gamma_{hole} = 1.2$ GHz. Thus the writing speed of the holeburning memory, 10 Gb/s, in principle, exceeds the speed of present commercial memories that may approach the 100 Mb/s - 1 Gb/s range. Here speed is given in terms of number of bits written per second.

5.1.4 High Temperature Cycling and Storage of Data

It is possible to cycle the holes to high temperatures. This is mainly due to the mechanisms of holeburning and the nature of the electron traps. Eu^{3+} traps, upon capturing the

electrons, transform into Eu^{2+} . The ground states of both Eu^{2+} and Eu^{3+} lie deep in the band gap, Figure 16B. Thermal excitations, even at room temperature, cannot release any electrons to the conduction band, as $k_B T \ll E_{i1}$ and E_{i2} , the energy differences between the ground states and the conduction band for Eu^{2+} and Eu^{3+} respectively. Holeburning is due to the redistribution of Eu^{2+} and Eu^{3+} in the lattice by photo-ionization. At cryogenic temperatures, where the lattice ions cannot move in response to the changing coulomb fields, the lattice is unstable and the holes are permanent. In such a system the erasure of holes would occur at high temperature where readjustment of Mg^{2+} and S^{2-} ions in response to the changing coulomb field is possible. Figure 17A shows the data on loss in holeddepth upon cycling the holes to higher temperatures for a few minutes and then reading at low temperatures.

There is no change in holeddepth and shape up to 150 K. However, in Figure 17B the raw data shows a $\sim 13\%$ loss in holeddepth upon cycling to 170 K. At this temperature the readjustment of the lattice has started. This feature is very favorable for storing the information at high temperature, especially above 77 K, liquid nitrogen temperature. To reconfirm the possibility of high temperature storage, holeburning data was stored for more than one day at 100 K, and no losses in holeddepths were observed.

5.1.5 Fast Optical Erasure

Fast optical erasure of memory is possible in MgS:Eu . This is unlike many photon-gated photo-ionization holeburning materials where heating the samples is required for erasure. The process of erasure, like that of holeburning, is also a resonant two-photon ionization process. However, in the erasure process, short-lived, broad vibronic states associated with 4f-5d transitions are involved. Such transitions have homogenous broadening, $\Gamma_h \sim 10\text{-}100$ THz. As a result, electrons from all Eu^{2+} centers can be excited via the vibronic band to the conduction band, wherefrom a redistribution of electrons reestablishes an equilibrium of charges and erases the holes. Erasure times down to 1 ms have been demonstrated. Several particularly attractive features of this photo-erasure process should be noted:

1. The erasure time should in principal be in the picosecond range. It is the duty cycle of the excitation process and the subsequent capture of electrons that limits the erasure time.

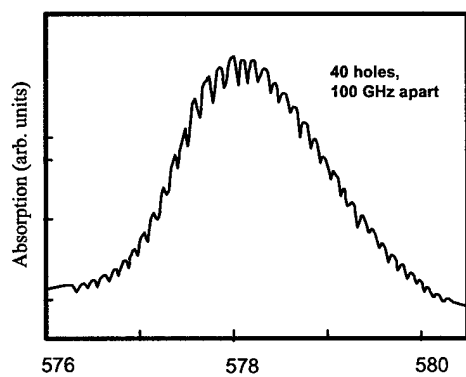


Figure 16A. Nanosecond Holeburning

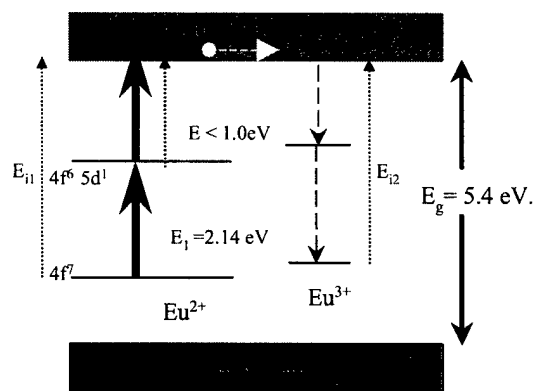
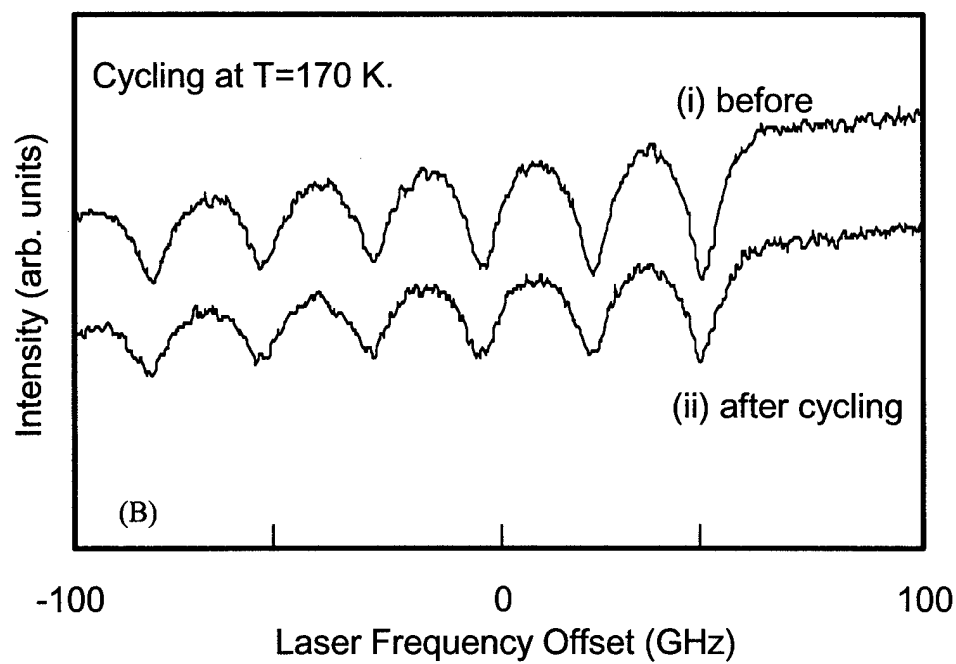
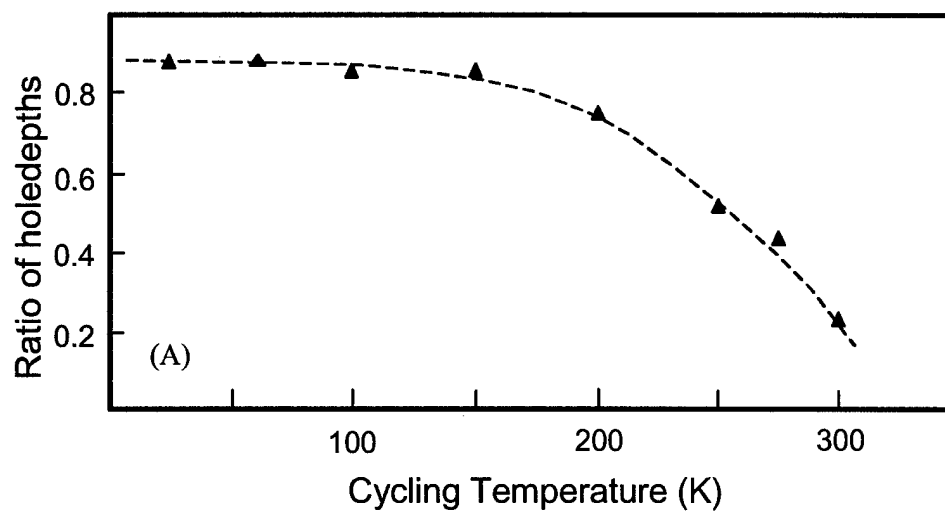


Figure 16B. Energy Levels (dotted arrows) & PGHB (red arrows) in MgS:Eu^{2+}



Figures 17A & 17B. Thermal Cycling of the Holes in MgS:Eu

2. Photo-erasure does not require the sample to be heated, which is a time consuming and inefficient process, especially at cryogenic temperatures.
3. Optical erasure is selective, as opposed to erasure by heating of the sample. Memory at every spatial location can be erased independently by focusing the erasure beam onto a particular spot. Therefore, in a practical device where a thousand holes are burned in a ZPL, for example, only a thousand bits would have to be erased simultaneously

5.1.6 Low Photon Budget

The low photon budget for writing and reading is due to two reasons:

1. As $\Delta l = 1$ for the holeburning transitions, a smaller photon budget will be required for reading the holes. For burning, both transitions, 4f-5d and 5d to conduction band, are electric dipole allowed. Therefore, burning is also very efficient. For 4f-5d transitions of MgS:Eu, Figure 15, the oscillator strength $f \sim 0.01$. This should be compared with the f-f transition where $f \sim 10^{-6} - 10^{-11}$.
2. The DWF is very large for the 4f-5d transition particularly in MgS:Eu where its value approaches the ideal value of unity (DWF=0.95). This implies that a very small fraction of the incident reading or writing beams will be absorbed by the vibronic band and wasted as heat.

5.1.7 Temperature Dependence

The most serious limitation on high-density spectral storage is its operation at cryogenic temperatures. As the temperature increases, the phonon broadening of spectral holes increases. This reduces the density of the holes possible. At 77K, for example, only 10-12 holes can be burned in the zero phonon line of MgS:Eu, whereas in excess of 1000 holes can be burned at ~ 10 K. The dependence of holewidth on temperature is shown in Figure 18. The experiments were performed in the following sequence: Spectral holes were initially burned at $T_{\text{burn}} = 2$ K. Subsequently, the temperature of the sample was raised to the pre-selected values, $T_{\text{read}} = 2-60$ K, at which the traces of the spectral holes were recorded. Holewidth did not change significantly for temperatures up to 20 K. As can be seen in Figure 18, above 20 K, the holewidth increased

rapidly with temperature. In this series of experiments, the holes became too broad above 60 K to be detected in the range of the dye laser scan.

Our data on MgS:Eu^{2+} indicates that holewidth remains constant up to 20 K. It then follows a temperature dependence of the holewidth proportional to $T^{1.5}$. This weak T-dependence is typical for rare earth doped glasses and has been explained in terms of two-level system and local modes. CaS:Eu also exhibits temperature dependence similar to MgS:Eu ^{26,29-31}.

It should be noted that ultra-high density storage in this system can be achieved up to 20 K. This temperature is an order of magnitude higher than what is necessary for high-density storage in f-f transitions that have been conventionally used for holeburning memories in the past.

5.2 Ultra-High Density Storage in Thin Films

All of the data presented above were for holeburning in MgS:Eu microparticles. For any practical device such particles cannot be used. A two-dimensional or three-dimensional medium is required for any practical device. For this reason, a complete experimental program of fabricating thin film and multi-layer structures by Laser Pulsed Vapor Deposition was initiated. A delicate atomic engineering of such structures was needed to observe power-gated holeburning with high efficiency, high density, and fast speed. Fabrication of thin films has been described in methods previously^{20,32}. Here we present the data on holeburning that is most relevant to spectral storage.

In order to compare the performance of thin films with microparticles, a large number of holes were burned in MgS:Eu films. Holeburning experiments were performed for two different centers of Eu in MgS: i) the normal Eu center that is formed in MgS powders, and, ii) an oxygen charge-compensated center that can be formed if growth takes place in the presence of oxygen. The oxygen ion goes as O^{2-} in the MgS lattice substituting for S^{2-} . If this substitution is around a Eu^{2+} ion, it will shift its energy levels. One strongly absorbing Eu^{2+} center is formed this way. The ZPL for this center lies at 588 nm, quite separated from the ZPL of the normal MgS:Eu center which is located at 578 nm. Figure 19A and 19B show the emission spectra of two such samples. Efficient holeburning was possible in the oxygen compensated center as well. Figure 19C shows 400 holes burned in its ZPL. In the normal Eu center 360 holes were burned to

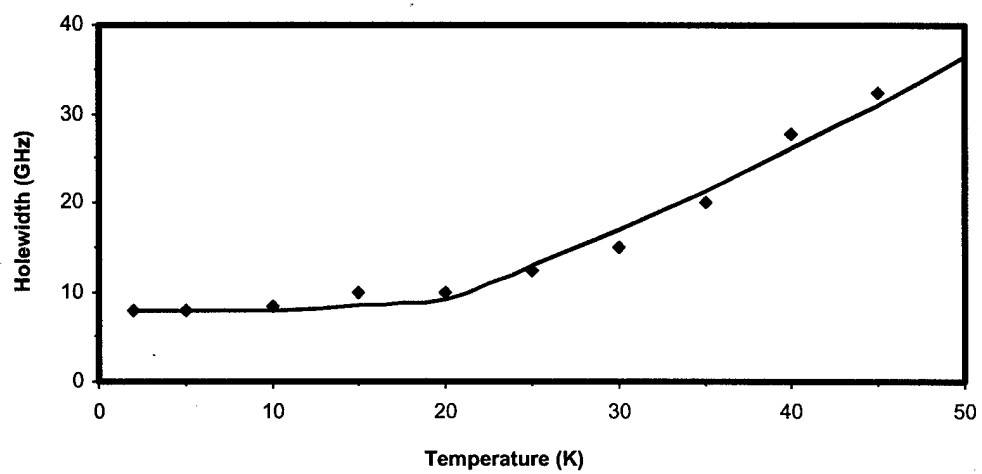


Figure 18. Temperature dependence of the holes in MgS:Eu powder

demonstrate the high density of holeburning, Figure 19D. The holes were burned at $T = 2$ K and with a beam power of 100 mW. The typical burning time with a cw laser was 2 seconds, and the typical width of the hole was $\Gamma_{\text{hole}} \sim 10$ GHz. The oxygen compensated center had all other holeburning characteristics as good as those in the normal center. Furthermore, the ZPL in the oxygen compensated center was broader than that of the normal center as shown in Figure 19.

5.2.1 Ultra-High Density Storage in Multi-Layer, Multi-Center Structures

Multi-layer structures with different materials and/or different optical centers were fabricated using the LPVD setup developed in-house (Figure 8). Three different materials were deposited to demonstrate the strength of storage multiplexing in multi-layer structures. By introducing traces of oxygen in the growth chamber, a new oxygen associated center of MgS:Eu could be created. The ZPL of this material lies at 589 nm. In one structure layers of CaS:Eu, MgS:Eu, and MgS:Eu + O were deposited. The typical thickness of the layer was 1μ . A buffer layer of ZnS separated these layers in order to stop any diffusion across them. ZPL's of 4f – 5d transitions of Eu^{2+} in these layers of MgS, CaS, and oxygenated MgS lie at 575, 625 and 589 nm, respectively. All three centers show efficient holeburning and have been deposited in layers over each other, Figure 20.

Holeburning in multi-layer structures is shown in Figure 21. The Γ_{inh} of the three ZPL's are such that in all 3000 holes could be burned in one physical location in this three-layer three-center structure. This multiplies the storage density by the number of layers, i.e. 1000 holes per layer. Storage in multi-layer structures has introduced a totally new concept in three-dimensional optically addressable spectral memories. Multi-layer, multi-center storage has many advantages:

1. In every micron or so thick layer a thousand bits can be stored.
2. Each layer contains a different optical center involving different RE atoms. Therefore, demands on material performance are greatly reduced as compared to single layer storage with a similar density.
3. In each layer, holes are burned at a different energy, i.e., in the range of the ZPL of each center. Therefore, storage in multi-layer structures provides independently addressable memories in different frequency ranges. This allows for parallel writing and reading,

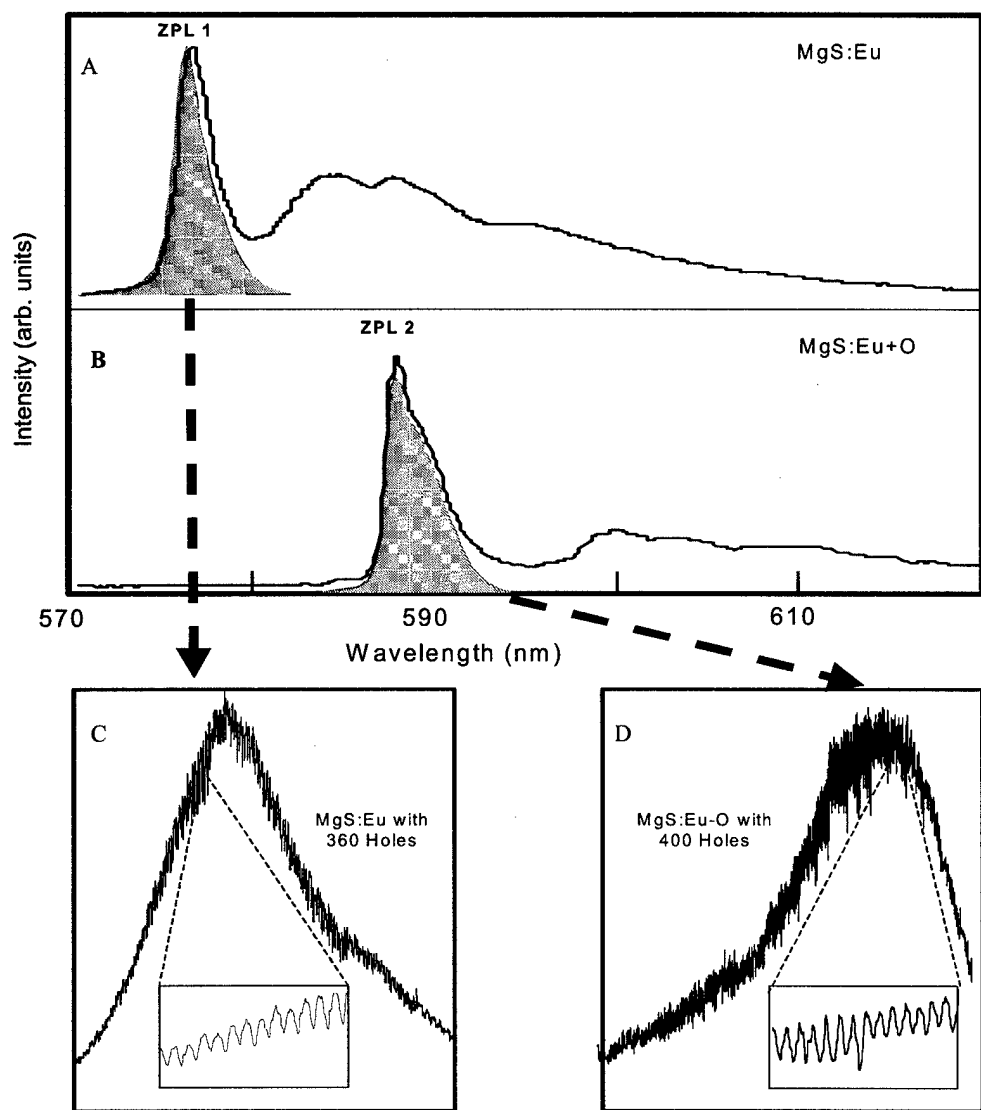


Figure 19. LPVD thin films: (A) and (B) ZPL's of MgS:Eu and MgS:Eu+O centers in emission respectively; (C) and (D) Ultra dense holeburning in MgS:Eu and MgS:Eu+O ZPL's

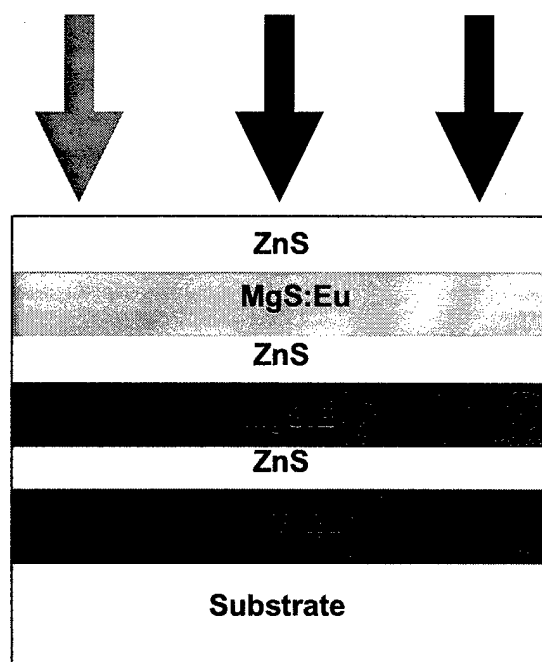


Figure 20. Multi-layer Structures and Their Possible Parallel Addressing

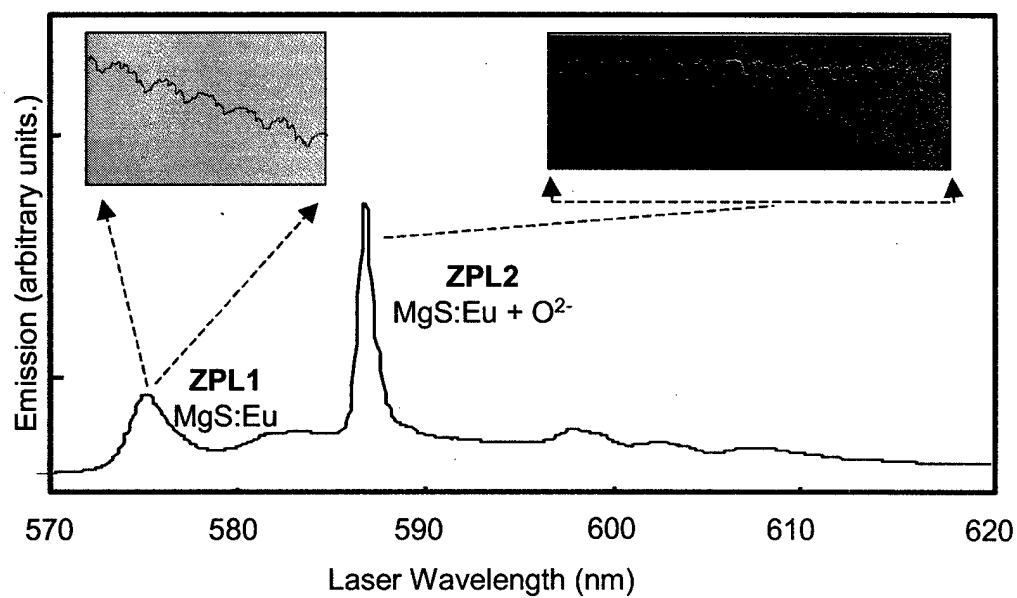


Figure 21. Ultra-high Density Multi-layer Storage in MgS:Eu and MgS:Eu + O

and hence a faster speed for both. Figure 20 shows schematically the parallel optical addressing possible with different color beams in such structures.

4. In these multi-layer structures, a further selectivity of erasure is possible. Spectral memories in these structures can be separated into various bins, each corresponding to a layer where the information is stored in a distinctly different region of the spectrum. Optical erasure allows the information in each layer to be erased independently by simply frequency tuning the erasure beam.

It is anticipated that other interesting applications of such multi-layer and optically independently addressable structures will be found in photonics and quantum electronics.

5.3 Mössbauer Studies

In principle, for samples containing Eu, the ratio of $\text{Eu}^{2+}/\text{Eu}^{3+}$ can be determined by Mössbauer measurements. However, for low concentration samples ($\text{Eu} \sim 0.01$ mol %) that are used for spectral holeburning, such experiments are very challenging. Mössbauer experiments require very long data accumulation times at such low concentrations of Eu. Figure 22 shows the Mössbauer spectrum of $\text{Eu}^{2+}/\text{Eu}^{3+}$ in a typical microparticle MgS sample with 0.01 mol % Eu. The accumulation time for the data was five days. The ratio of the concentration of two valence states, $\text{Eu}^{2+}/\text{Eu}^{3+}$ can be determined from the ratio of the areas under the respective Mössbauer signals.

5.4 MgS:Eu Embedded in Different Hosts

The large inhomogeneous broadening of the 4f-5d transition allows for a high density of storage in MgS:Eu. Γ_{inh} for this transition is ~ 1.6 nm for 0.01 % molar concentration of Eu. The linewidth in pure crystals is not very different from that in polycrystalline powder. For example, in CaS:Eu the linewidth in the single crystal is ~ 2 nm which is comparable to that of the powder, ~ 0.8 nm^{33,9}. This indicates that the broadening is due to the inherent charge compensation effects that are essential when MgS is doped with Eu, particularly in the form of Eu^{3+} . Such atomic scale defects will give a broadening that will not differ from a polycrystalline system to a single crystal.

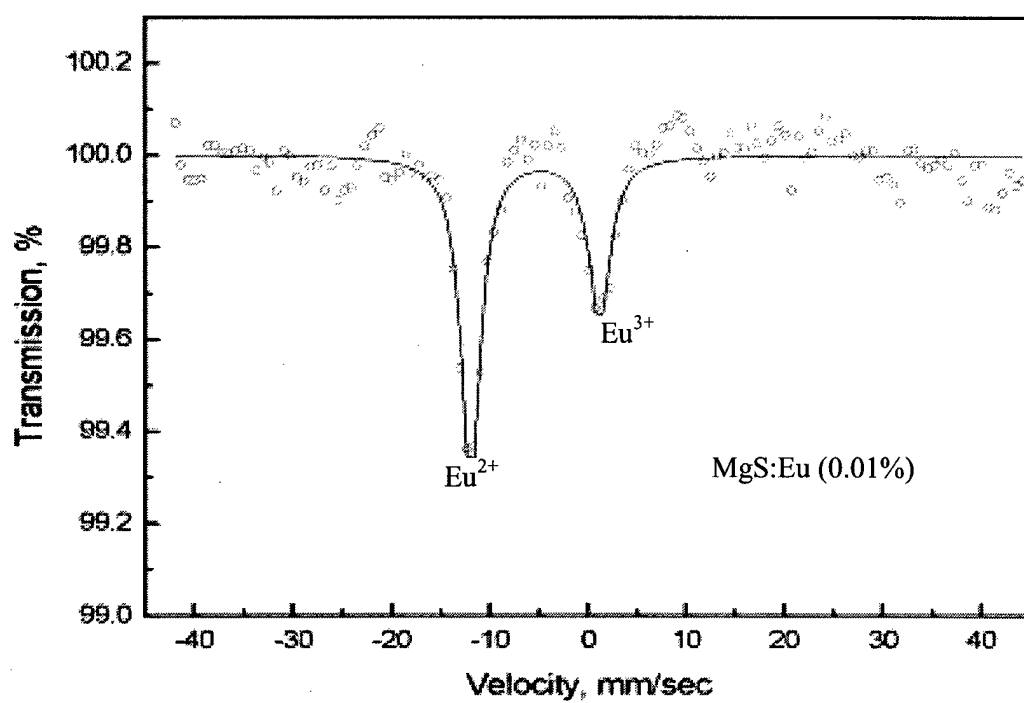


Figure 22. Mössbauer spectrum of MgS:Eu indicating the ratio, $\text{Eu}^{3+}/\text{Eu}^{2+}$.

Microparticles of MgS:Eu were imbedded in different hosts i.) to further enhance the Γ_{inh} and hence the storage density, and ii.) to change the electron-phonon coupling so as to increase the operational temperature of the spectral storage.

5.4.1 High-Density Holeburning in MgS:Eu in Polymers

Embedding MgS:Eu particles in PolyMethyl Methacrylate (PMMA) enhanced Γ_{inh} without sacrificing Γ_h , i.e., the holes burned in the MgS:Eu embedded in polymers had the same holewidth as those in the powder at the same burn temperatures. Figure 23 shows the hole burned in MgS:Eu in PMMA matrix³⁴. This indicates that a proportionately larger number of holes can be burned in the ZPL of MgS:Eu in PMMA. It has been shown that the inhomogeneity of the environment can further be increased so as to increase Γ_{inh} by as much as a factor of five.

Molecular Weight Dependence: A set of samples was prepared by embedding microparticles of MgS in PMMA with five different molecular weights ranging from 12,000 to 996,000. The resulting spectra are shown in Figure 24. The ZPL becomes broader and DWF becomes smaller for the samples embedded in the longer chains.

The ZPL of MgS:Eu in PMMA is broadened to many times its value in the powder sample. Such increased Γ_{inh} would lead to a larger number of holes in the ZPL. The ZPL of MgS:Eu in comparison to that of MgS:Eu in PMMA is shown in Figure 23. In a small portion of the ZPL, 160 spectral holes 25 GHz apart were burned at 10 K. Burning power levels of 100 mW/cm² and exposure times of 1 s were used during the multiple holeburnings. The spectral holes had typical holewidths of 11 to 12 GHz. A very important feature of the enhancement of the ZPL is that the material retained its excellent holeburning properties. The spectral holes burned had the same holewidth and holeshape. Therefore, a higher density of spectral holes is possible with this enhanced broadening. Thus, in excess of 1000 holes per spatial location can be achieved.

Although the ZPL is broadened and the density of the spectral holes is increased, there are still three major limitations to be considered in PMMA embedded samples. First, since the index of refraction for MgS and PMMA are different, laser beams scatter between these two media. Thus, the efficiency of holeburning is reduced in the PMMA host. Second, the concentration of the optically active Eu²⁺ ions is reduced when it is embedded in PMMA.

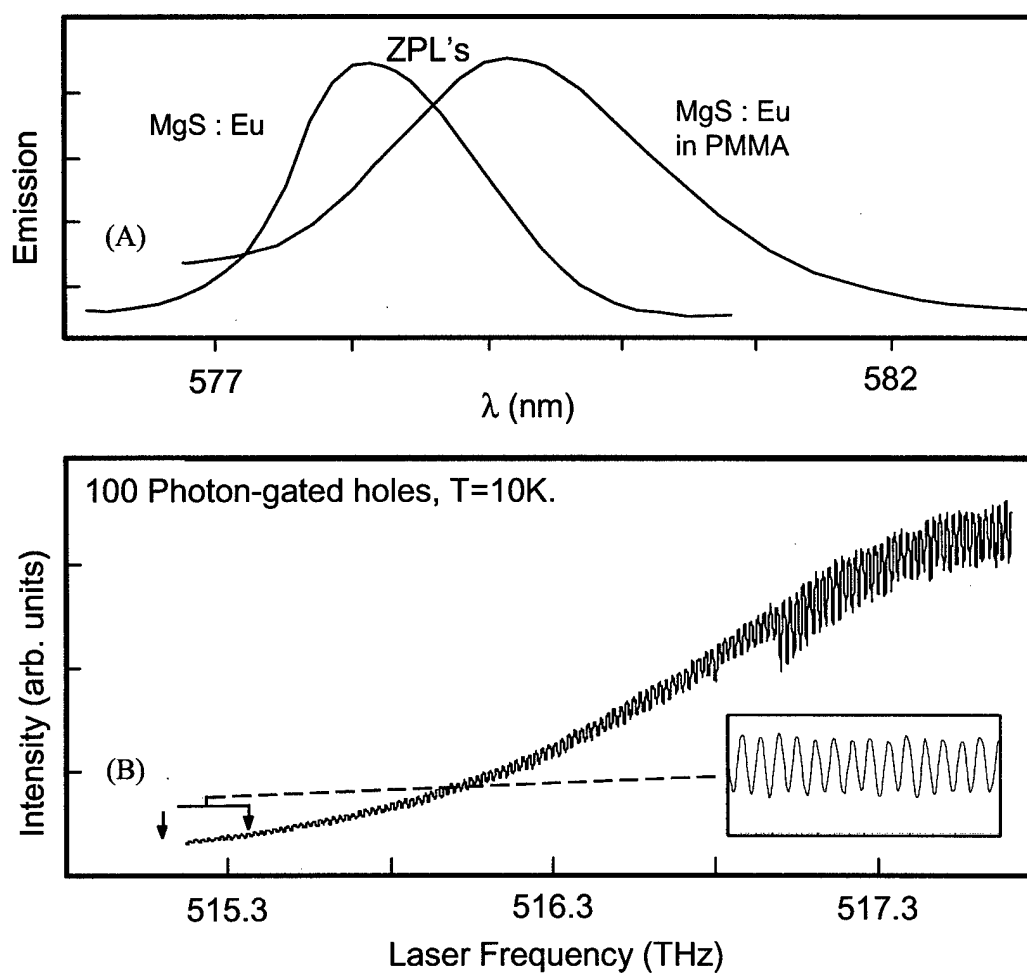


Figure 23. ZPL's of MgS:Eu Microparticles in powder and in PMMA (A),
Ultra-High Density Holeburning in MgS:Eu embedded in PMMA (B)

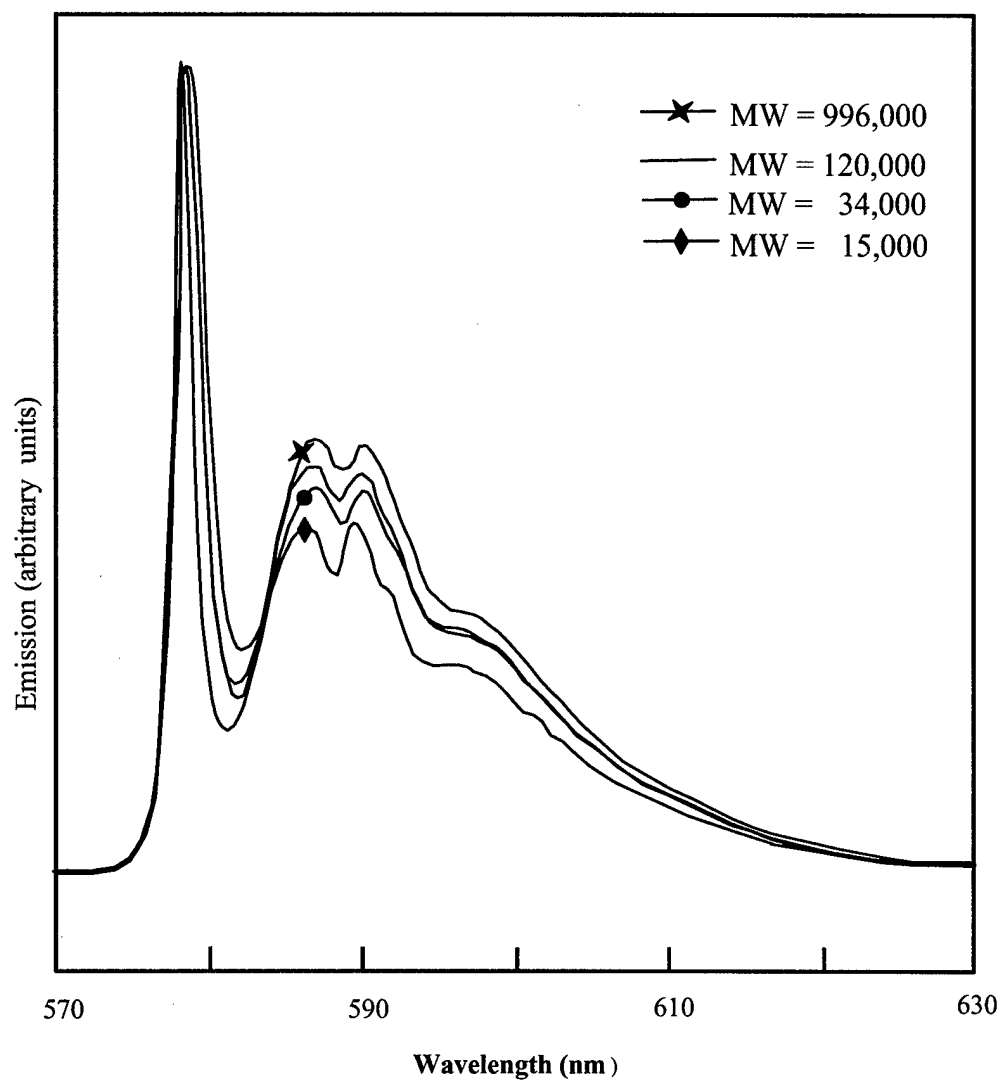


Figure 24. Molecular weight dependence on the linewidth of the ZPL.

Therefore, the number of Eu^{2+} ions available for holeburning is also reduced. A consequence of this is an increase in the power required for burning and reading the holes. Third, in the PMMA host electron-phonon coupling is increased. This increases the holewidth as compared to the powder samples at any temperature.

5.5 Holeburning in Nanoparticles

Nanoparticles of MgS:Eu were grown by pulsed laser vapor condensation. The resulting material had a high ratio of Eu^{2+} to Eu^{3+} ions. The ZPLs as well as spectral holes burned in the nanoparticle samples were broader than those of microparticles, Figures 25 & 26. Due to the enhanced broadening of the ZPL in nanoparticles, the number of possible spectral holes had been increased. Large inhomogeneous broadening could be attributed to the size distribution of the nanoparticles and their large surface to volume ratio that allows for more inhomogeneities. Spectral holewidths showed strong temperature dependence in nanoparticles, which is attributed to an enhancement in electron-phonon interaction due to size confinement. Similar effects have been observed in other systems.

In nanoparticles, the holes are generally broader and this broadening rapidly increases with temperature. Therefore nanoparticles as such are not suitable for high-density spectral storage when compared to microparticles or thin films²².

5.6 Temperature Dependence in Different Hosts

The biggest drawback of high-density data storage is the broadening of the hole at elevated temperatures. This rapidly decreases the storage density to insignificant amounts. The temperature dependencies of the holewidths in MgS:Eu microparticles, microparticles embedded in PMMA, and MgS:Eu nanoparticles were studied and compared³⁵⁻³⁸. The objective was to raise the operational temperature of the high-density holeburning storage by changing the phonon spectrum of the medium and the electron-phonon coupling.

The holes start to deteriorate at lower temperatures in PMMA embedded samples than in microparticles. The temperature dependence of the holes for the powder was found to be proportional to $T^{1.5}$. On the other hand, the PMMA matrix increases the power of the T dependence. The dependence for the 34,000 and the 120,000 molecular weight PMMA is $T^{1.6}$

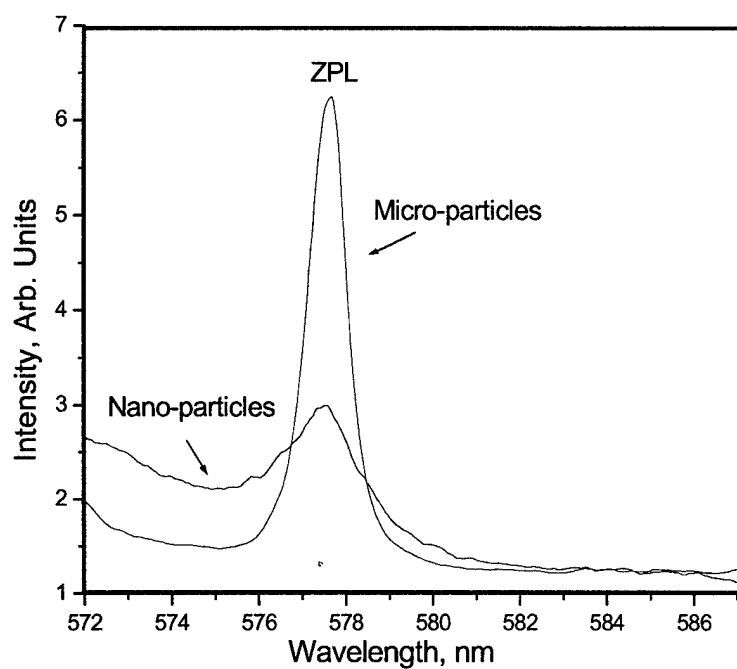


Figure 25 Excitation Spectrum MgS:Eu in Nanoparticles

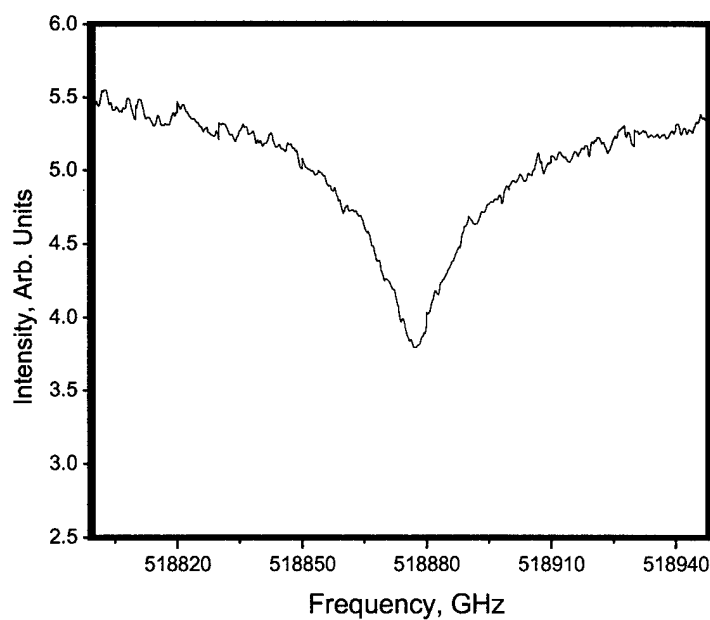


Figure 26. Persistent Spectral Hole-burning in MgS:Eu Nanoparticles

and $T^{2.1}$ respectively, Figure 27. Therefore, PMMA increases phonon coupling and plays a critical role on the temperature broadening of the holes.

The data showing the temperature dependence of holewidth in nanoparticles is presented in Figure 28. As the samples were mixed microparticles and nanoparticles, data was compared with the data on pure microparticles samples under the same conditions. It was found that the holes burned at all temperatures, 2-25 K, had two components: 1.) Narrow component that followed the temperature dependence of the holes burned in microparticles, found in the lower trace, and 2.) Another very distinctly broad component of the hole, which showed much stronger dependence on temperature. This component was attributed to nanoparticles. These two contributions to the hole were extracted by curve fitting two Lorentzians to the holeburning spectrum.

From the traces in Figure 28, it is evident that there are two temperature regions. At low temperature the holes in microparticles samples show minimal broadening up to 25 K. Beyond this temperature, the holewidth increases rapidly. For nanoparticles, the holes are generally broader at any constant holewidth. The increase of holewidth with temperature is much more pronounced for microparticles. Such enhanced broadening of holes in nanoparticles is an indication of stronger electron-phonon coupling. This result has also been observed by other researchers and has been attributed to the increased atomic motion at the surface of the nanoparticles. A systematic study of the holewidth in nanoparticles with the separation of nanoparticles and microparticles would be necessary before making a detailed comparison. However, it is clear that in nanoparticles the holes are generally broader. The increase in holewidth with temperature is faster in nanoparticles than in microparticles. Broader holes in nanoparticles means that nanoparticles will have a significantly lower density of spectral storage as compared to microparticles and thin films.

5.7 II-VI Materials Doubly Doped with Rare Earths

The main source of the electron traps in MgS:Eu is Eu^{3+} ions. Although the concentration of Eu^{3+} in MgS is high and they form deep traps, once Eu^{3+} captures the electron, it becomes Eu^{2+} . This Eu^{2+} will have its absorption randomly located inside the ZPL. Therefore, burning more holes results in the partial filling of the spectral holes already burned in the ZPL. This results in lower efficiency of burning. Double doping of the MgS:Eu with Sm was

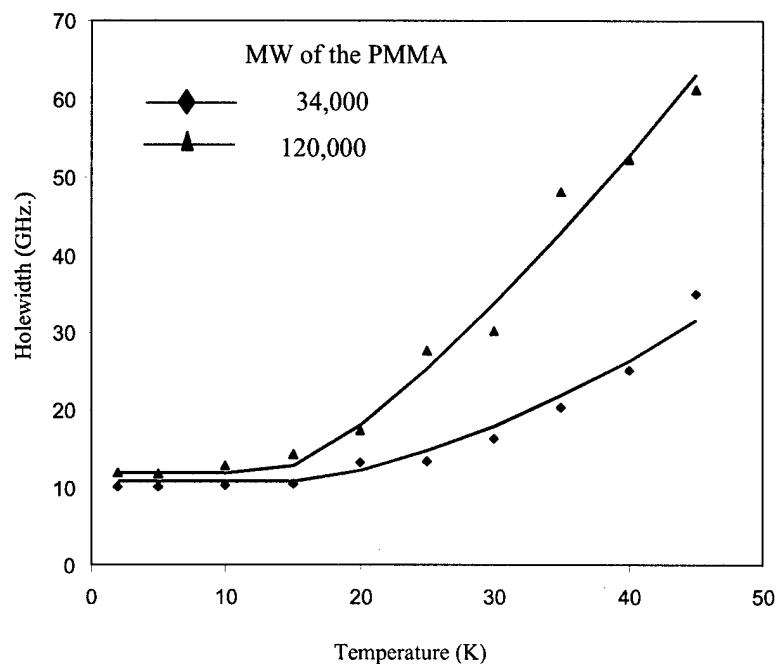


Figure 27. Temperature dependence of the holewidth, MgS:Eu in PMMA

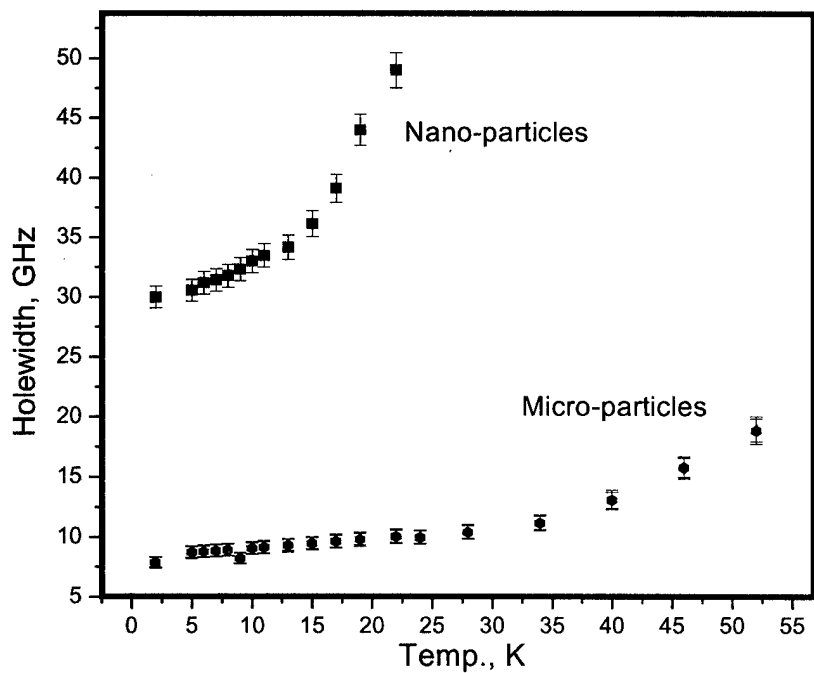


Figure 28. Temperature dependence of the holewidth, MgS:Eu in micro and nano particles.

investigated to create traps other than Eu^{3+} . Sm was chosen over the other rare earth ions due to the fact that with the exception of Eu, it is the only rare earth ion that is stable, as Sm^{2+} and Sm^{3+} . It was hoped that the capture of Eu^{2+} electrons liberated in the holeburning process by Sm^{3+} may increase the efficiency of spectral holeburning and may prevent the partial filling of the spectral holes already burned during the multiple holeburning process.

Double doped MgS with Eu and Ce was also used for holeburning. Ce in solids can exist as Ce^{3+} and Ce^{4+} as the 4f shells becomes completely empty and stability is attained. Like the doubly doped MgS with Sm and Eu samples, the Eu and Ce doubly doped samples showed the identical $\text{Eu}^{2+} 4f - 5d$ transition in emission and absorption.

5.7.1 Holeburning in MgS:Eu,Sm

Double doped samples of MgS with Sm and Eu were used for holeburning. The $\text{Eu}^{2+} 4f^7 - 4f^6 5d^1$ spectrum in the double doped sample is essentially the same as in the singly Eu doped sample. This confirmed that Sm and Eu do not occur as pairs in MgS, and Sm^{2+} and Sm^{3+} are randomly distributed in the solid. However, in holeburning experiments performed in the doubly doped system, the burning efficiency, holedepth, holewidth, and sensitivity to temperature were all found to be the same as for the singly doped samples. This suggests that Sm does not play any significant role as far as holeburning characteristics are concerned.

The presence of Sm^{3+} has been established by our spectroscopic data and by other work on thermoluminescence and photo-luminescence³⁹. The result on holeburning can be explained if the Sm^{2+} ground state is very close to the conduction band. In this case as the electrons during the holeburning process are created, a fraction of them will be captured by Sm^{3+} ions. The probability of the capture of the electron by Sm^{3+} would not be very different than that of Eu^{3+} . On the other hand, electron capture is not permanent. It is known that the Sm^{3+} ground state is quite deep, $> 2\text{eV}$, in the band gap. However, upon capture, Sm^{3+} converts to Sm^{2+} , which lies very close to the conduction band. It will quickly loose its electron to the conduction band in the presence of the burning beam or otherwise when thermally excited. This interpretation is supported by the thermoluminescence and photo-luminescence data of Mathur³⁹.

5.7.2 Holeburning in MgS:Eu,Ce

Like MgS:Eu,Sm, holeburning investigations were performed on double doped MgS:Eu,Ce samples. It was observed that the erasure of the previously burned holes upon multiple holeburning was noticeably different in doubly doped systems than in the singly doped Eu samples. Two holes were burned consecutively under the same conditions in the MgS:Eu (0.05 % mol. Eu) and MgS:Eu,Ce (0.05% mol. Eu and 0.05 % mol. Ce) samples. As shown in Figure 29, burning the second hole decreases the holeddepth of the first hole burned earlier. However, singly doped Eu loses 50% of the original holeddepth, while doubly doped MgS with Eu,Ce only loses 25% of the original holeddepth. This clearly indicated that in addition to the Eu^{3+} , Ce^{4+} is also acting as a trap for the electrons released from Eu^{2+} in the holeburning process. Upon capturing Ce^{4+} , it becomes Ce^{3+} . These electrons cannot be released back to the conduction band from Ce^{3+} since it acts as a deep trap. Ce^{3+} and Ce^{4+} do not absorb in the region of the ZPL of Eu^{2+} in MgS⁴⁰.

5.8 $\text{Al}_2\text{O}_3:\text{Ti}^{3+}$

The objective of the experiments reported here was to use Ti^{3+} photo-ionization photon-gated holeburning in $\text{Al}_2\text{O}_3:\text{Ti}^{3+}$. This material has been of interest for optical studies since it is a broadly tunable solid-state laser material for the near infrared spectral region (0.7-1.1 μ). Optical studies have shown that Ti^{3+} as well as Ti^{4+} exist in this crystal. Ti^{3+} ($3d^1$) substitutes Al^{3+} and is surrounded by an octahedron of oxygen ions with a slight trigonal distortion. Two types of Ti^{4+} ions (locally and non-locally charge compensated) are identified optically⁴¹. It was known that Ti^{3+} can be ionized by single and two-photon ionization.

Professor McClure of Princeton University provided the samples used. The crystals were 2-3 mm thick and polished on two sides. The concentrations of Ti^{3+} and Ti^{4+} have been measured in earlier studies^{41,42}.

Power-gated holeburning in this material was not possible as the band gap is very large. Photon-gated holeburning was tried in several different experimental setups.

The cw setup was used for holeburning. The high-resolution laser was used as the source of the reading photons. An excimer laser at $\lambda = 308$ nm or a range of wavelengths (300-400 nm) from an argon ion laser were used as a source of gating photons.

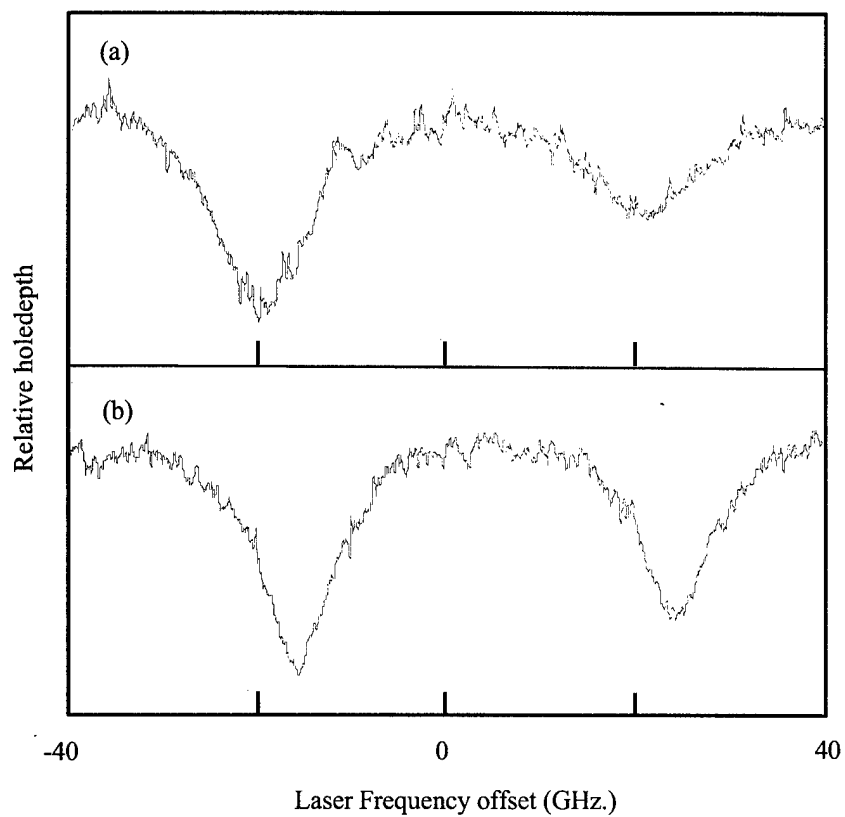


Figure 29. Deep holes burned in MgS:Eu (a) and MgS:Eu+Ce. The effect of reduction in erasure can be readily seen in the doubly doped system.

In both of these cases, no detectable holes were observed. However, an overall bleaching of the line was observed, Figure 30. At the same time, it was not possible to reverse the holeburning process so as to recover the Ti^{4+} traps for subsequent experimentation.

Overall bleaching of the ZPL can be explained as follows. The photo-ionization of Ti^{3+} - Ti^{4+} has been experimentally demonstrated by different techniques. However, photo-ionization creates time varying Coulomb fields. Such fields Stark shift the energy levels of Ti, bringing the entire set of Ti^{3+} ions in resonance with the laser. Since Ti^{3+} is a $3d^1$ ion, the energy levels of Ti^{3+} are extra sensitive to the time varying Coulomb fields. This way, the spectral hole can be broadened to cover the entire Γ_{inh} , especially when long burning times are involved. Hence, an overall bleaching of the ZPL for long exposure times can be explained.

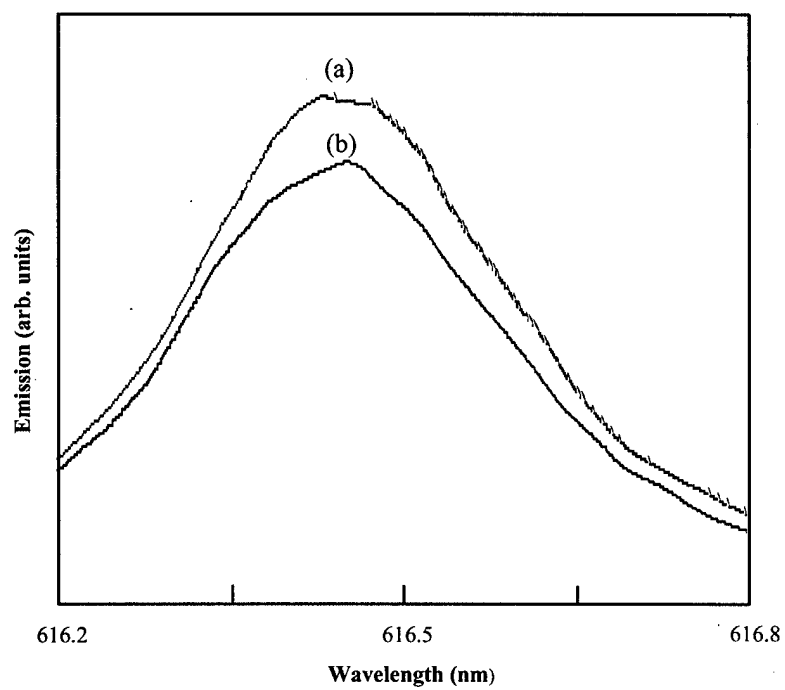


Figure 30. Bleaching of the entire ZPL of Al_2O_3 (a) before and (b) after the holeburning.

6. Conclusions

Spectral holeburning based memories have been investigated for the last quarter century or more. No viable holeburning based device has been realized so far. Recent breakthroughs have warranted a fresh look at the potential for the realization of holeburning devices. In particular, the principal investigator at Temple University has developed novel rare earth (RE) doped II-VI materials and fabricated their thin film, multi-layer, and nano-structures. These materials were designed to exhibit a new kind of gated-holeburning, specifically, power-gated holeburning. This technique has demonstrated the potential of these materials for fast and ultra-dense spectral storage. The salient features of these spectral storage materials are.

1. In multi-layer thin film structures, ultra-dense spectral storage with several thousand bits of memory per focused laser spot is possible. This increases the density of persistent holeburning based storage by three orders of magnitude.
2. Nanosecond storage in microparticles and thin film structures has been demonstrated. This increased the storage speed by six to seven orders of magnitude.
3. The reading and writing of holeburning memory is highly efficient approaching the theoretical limits.
4. This memory is optically erasable and allows for multiple rewrites. Erasing times as short as milliseconds have been established experimentally.
5. Possible long-term storage of memory at temperatures up to 150 K.
6. The minimization of optical losses and heating of the medium by phonons.
7. This memory survives optical cycling to high temperatures up to 150 K.
8. A high density of spectral holes up to a relatively high temperature, ~ 25 K. This is an order of magnitude improvement over the previously set limits, ~ 2 K, for media based on holeburning in rare earth f-f transitions.

This success is due to atomic engineering of transition energies, the strength of rare earth transitions involved in holeburning, and the appropriate tailoring of the II-VI host energy band structure. Rare earth 4f-5d transitions used for holeburning were ideally suited to atomic tailoring. In II-VI sulfides, the energies of f-d transitions are affected only moderately and

therefore can be adjusted within the desired region of the spectrum by going from one host to another.

Rare earth doped II-VI sulfides have not only outperformed other holeburning materials, but have set new standards in persistence, speed, high-density, and optical erasability. The most striking aspect of these ultra-dense memory materials is that their other performance parameters also meet or exceed the specifications of current technology. Having all performance parameters optimized in a single material makes spectral storage a very promising future technology.

In light of the above, it is obvious that the cryogenic temperature of operation is the biggest obstacle towards a successful implementation of spectral memories. Currently, the operational temperature of these materials is ~ 25 K, which is an order of magnitude better than the operational temperature of other materials at comparable storage densities. However, it is not high enough for many applications. Research on increasing this temperature limit is therefore very promising, especially in light of recent advances in thermoelectric and other compact solid-state coolers which are expected to make 30-50 K temperatures commonplace.

7. Recommendations

The research performed on rare earth doped II-VI materials has set the limit on high-density spectral storage by exploiting condensed matter at the atomic level. The best direction for future research would be to use the best-known POGHB materials with smart designs to maximize storage density together with all other characteristics of the holeburning medium. Research on such atomically engineered photonics materials would have a broad impact as many other applications of these multi-layer and nano-structures can be envisioned in photonics, integrated optics, and quantum electronics.

Despite the favorable characteristics discussed in the previous sections, there are limitations inherent in the materials with their current state. These limitations need to be addressed before this technology could be brought to the marketplace:

- The most serious limitation is the cryogenic temperature of operation that is necessary for high-density storage. Current cryogenic accessories are bulky, inefficient, and in general, very cost ineffective. There are, however, constant efforts to make more compact and efficient cryogenic coolers^{43,44}. If successful, these efforts would have a great impact on the practicality of the RE doped sulfides that operate at or below 25 K.
- An alternate approach avoiding cryogenic temperatures is the investigation and design of materials that can operate at higher temperatures. Developing materials that operate at room temperature or even at 77 K with a high density of spectral holes would be considered a major breakthrough.
- Initial observations support the idea that nanoparticles embedded in appropriate media may reduce the effect of electron-phonon coupling¹⁰, hence possibly providing a high-density, high-temperature storage medium. The holeburning properties of RE doped nanoparticles and embedded nano-materials should be investigated in detail, especially for high temperature burning.
- The inconvenient wavelengths of operation of the materials studied so far are another practical aspect to improve upon. These wavelengths fall in the red-orange region of the spectrum. Bulky liquid dye lasers are necessary for all optical investigations. Performance of holeburning materials in the IR region of the spectrum is very important. This will greatly reduce the cost as well as the size of any future device and would take

full advantage of developments in communication diode laser technology. Alkaline earth sulfides, oxides, and selenides, such as but not limited to, ZnS, ZnSe and ZnO should be the first few materials to be investigated for this purpose. All possible RE^{2+} - RE^{3+} and RE^{3+} - RE^{4+} combinations should be tried for photo-ionization holeburning in the near IR.

- The best systems tailored thus far are based on Eu doped materials. In Eu the hyperfine splitting of the ground state broadens the holes and is a limiting factor on the density of storage. Materials with RE ions that have zero nuclear spins or minimal hyperfine interaction, so as to allow for narrower holes and a high storage density, should also be investigated.
- It has been shown that thin film multi-layer structures of RE doped sulfides exhibit the highest density of spectral storage. Such multi-layer structures have many other potential applications. A major thrust of future research should be to improve upon the atomic tailoring and growth of these multi-layer structures.

8. References

1. A.A. Gorokhovskii, R.K. Kaarli, and L.A. Rebane, "Hole-burning in the contour of a pure electronic line in a Shpol'skii system," JETP Lett. Vol. 20, 216-218, 1974.
2. A. Szabo, "Frequency selective optical memory," U.S. patent 3,896,420 (22 July 1975).
3. G. Castro, D. Haarer, R.M. Macfarlane, and H.P. Trommsdorff, "Frequency selective optical data storage system," U.S. patent 4,101,976 (18 July 1978).
4. W.E. Moerner in "Persistent Spectral Hole-burning: Science and Applications" Springer-Verlag Topics in Current Physics, 1988.
5. T. P. Carter, C. Brauchle, V.Y. Lee, M. Manavi and W.E. Moerner, "Mechanism of Photon-Gated Persistent Spectral Hole-burning in Metal-Tetrabenzoporphyrin/Halomethane Systems: Donor-Acceptor Electron Transfer," J. of Phys. Chem. 91, 3998-4004, 1987.
6. B. Plagemann, F.R. Graf, S.B. Altner, A. Renn, and U.P. Wild, "Exploring the limits of optical storage using persistent spectral hole-burning: holographic recording of 12000 images," Applied Physics B, Vol. 66, 67-74, 1998.
7. Y.S. Bai, W.R. Babbitt, and T.W. Mossberg, Opt. Letters Vol. 11, 727, 1986, Also, H. Lin, T Wang and T.W. Mossberg, Opt. Lett. Vol. 20, 1658, 1995.
8. M.K. Kim, R. Kachru, Opt. Lett. Vol 12, 594, 1987, Also, X.A. Shen, E. Chiang and R. Kachru, Opt. Lett. Vol. 19, 1246, 1994.
9. Z. Hasan, M. Solonenko, P.I. Macfarlane, L. Biyikli, V.K. Mathur, F. A. Karwacki, "Persistent high density spectral hole-burning in CaS:Eu and CaS:Eu, Sm phosphors," Applied Physics Letters, Vol. 72, 2373-2375, 1998.
10. Z. Hasan, L. Biyikli, and P.I. Macfarlane, "Power-gated spectral hole-burning in MgS:Eu²⁺, Eu³⁺: A case for high-density persistent spectral hole-burning," Applied Physics Letters, Vol. 72, 3399-3401, 1998.

11. H.W.H. Lee, M. Gehrtz, E.E. Marinero and W.E. Moerner, "Two Color Photon-Gated Hole-Burning in an Organic Material," *Chemical Physics Letters*, Vol. 118, 611-616, 1985.
12. A. Winnacker, R.M. Shelby, and R.M. Macfarlane, "Photon-gated hole-burning: a new mechanism using two-step photoionization," *Optics Letters*, Vol. 10, July, 1985.
13. W. Denk, J.H. Stickler and W.W. Webb, "Two-Photon Laser Scanning Fluorescence Microscopy", *Science*, Vol. 248, 73-76, 1990.
14. G. Robertson, D. Armstrong, M.J.P. Dymott, A.I. Ferguson and G. L. Hogg, "Two-Photon Florescence Microscopy with a Diode Pumped Cr:LiSAF Laser," *Applied Optics*, Vol. 36, 2481-2483, 1997.
15. R Pandey, S. Sivaraman, "Spectroscopic properties of defects in alkaline-earth sulfides," *Journal of Physical Chemistry Solids*, Vol. 52, 211-225, 1991.
16. D.S. McClure, Z. Kiss, "Survey of the spectra of the divalent rare-earth ions in cubic crystals," *The Journal of Chemical Physics*, Vol. 39, 3251-3257, 1963.
17. S. Asano, "Analysis of the absorption spectra $4f^{N+1} \rightarrow 4f^N 5d-6s$ of rare-earth ions in the cubic field: I. General formula," *Solid State Physics*, Vol. 12, 4081-4093. 1979.
18. N. Yamashita, Sh. Fukumoto, S. Ibuki, H. Ohnishi, "Photoluminescence of Eu^{2+} and Eu^{3+} centers in CaS:Eu,Na phosphors," *Japanese Journal of Applied Physics*, Vol. 32, 3135-3139, 1993.
19. Z. Hasan and L. Biyikli, "Photon-Gated Hole-burning Materials: Direction in High Density Memory Storage," *Materials Science Forum* Vol. 315-317, 51-58, 1999.
20. J.L. Park, L. Biyikli, M.F. Aly, and Z. Hasan (1999) "Pulsed Laser Deposited Thin Films of Sulfides for High Density Memory Storage," *SPIE Proceedings on Advanced Optical Data Storage: Materials, Systems and Interfaces to Computers* Eds: Z. Hasan and P. Mitkas Vol. 3802, 206-212 1999.
21. M.F. Aly, L. Biyikli, S. Dardona, J.L. Park and Z. Hasan, "Thin Films of Sulfides for High Density Optical Storage by Photon-Gated Hole-burning," *SPIE Proceedings on Photonic Devices and Algorithms for Computing*, Vol. 4114, 182-188, 2000.

22. S. Dardona, L. Biyikli, R. Esposito and Z. Hasan "Spectral Hole-burning in MgS:Eu Nanoparticles," SPIE Proceedings on Three and Four-Dimensional Spectral Storage Vol. 4459, 364-371, 2001.
23. Z. Hasan and L Biyikli, "Mechanism of High Density Power-Gated Hole-burning in Eu^{2+} - doped Sulfides," Journal of Optical Society of America B, Vol. 18, 232, 2001.
24. Z. Hasan, "Material Challenges for Spectral Hole-burning Memories," SPIE Proceedings on *Adv. Opt. Mem. and Interfaces to Computer Storage*, eds: P. Mitkas and Z. Hasan, Vol. 3468, 154-164, 1998.
25. L. Biyikli, M. Solonenko, S.M. Ahmadyan and Z. Hasan "High Density Photon-Gated Hole-burning in Sulfides," SPIE Proceedings on *Advanced Opt. Mem. and Interfaces to Computer Storage*, Eds: P. Mitkas and Z. Hasan, Vol. 3468, 285-292, 1998.
26. Levent Biyikli PhD thesis Temple University, unpublished, 1999.
27. L.Biyikli and Z.Hasan (to be published).
28. W.E. Moerner, T.P. Carter, C. Brauchle, "Fast burning of persistent spectral holes in small laser spots using photon-gated materials," Applied Physics Letters, Vol. 50, 430-432, 1987.
29. K.K. Rebane, "Impurity Spectra of Solids" NY-London: Plenum Press, 1970.
30. M. Solonenko Ph.D. Thesis Physics Department, Temple University, 1999.
31. M. Solonenko and Z. Hasan (to be published).
32. M. Aly, L.Biyikli, J.L.Park and Z.Hasan (to be published).
33. Basun, S.A., Raukas, M., Happek, U., Kaplyanskii, A.A., Vial, J.C., Rennie, J., Yen, W.M., Meltzer, R.S. (1997). Off-resonant spectral hole burning in CaS:Eu by time-varying Coulomb fields. Physical Review B, 56, 12992-12997.
34. S. M. Syedahmedian, M.F. Aly, L Biyikli, J.L Park, M. Solonenko, and Z. Hasan, "Inhomogeneous Broadening and Gated Hole-burning in MgS: Eu and CaS:Eu in Polymethyl-methacrylate (PMMA) ," J. Lumin. 84, 389-392, 1999.

35. L. Biyikli and Z. Hasan, "The Dynamics of Hole-burning in $4f^n-4f^n5d^1$ Transition of Eu^{2+} in MgS," *J. Lumin.* **83**, 373-377, 1999.
36. Biyikli, L., Solonenko, M., Ahmedyan, S.M., Hasan, Z. (1998). High Density Photon-Gated Holeburning in Sulfides. *Proceedings of SPIE*, **3468**, 285-292.
37. L. Biyikli and Z. Hasan to be published.
38. M. Solonenko and Z. Hasan (to be published).
39. K. Chakrabarti, V.K. Marthur, F. R. Joanne Abundi, R.J. (1988). Simulated luminescence in rare earth doped MgS. *J. Appl. Phys.*, **64**, 1363-1366.
40. M.F. Aly, L. Biyikli, S. Dardona, and Z. Hasan "High Density Frequency Domain Storage in Alkaline Earth sulfides Double-Doped with Lanthanides," *SPIE Proceedings on Photonic Devices and Algorithms for Computing*, Vol. 4114, 262-268, 2000.
41. W.C. Wing, D.S. McClure, S. A. Basun, M.R. Kokta, "Charge-exchange processes in titanium/doped sapphire crystal. Charge-exchange energies in titanium/bond excitation," *Physical Review B*, Vol. 51, 5682-5692, 1995.
42. W.C. Wing, D.S. McClure, S. A. Basun, M.R. Kokta, "Charge-exchange processes in titanium/doped sapphire crystal. Charge-transfer transition states, carrier trapping, and detrapping," *Physical Review B*, Vol. 51, 5693-5698, 1995.
43. R. Venkatasubramanian, E. Siivola, T. Colpitts, and B. O'Quinn, "Thin-film thermoelectric devices with high room-temperature figure of merit," *Nature*, Vol. 413, 597-602, 2001.
44. C. B. Vining, "Semiconductors are cool," *Nature*, Vol. 413, 577-578, 2001.

9. Symbols, Abbreviations, and Acronyms

D_q	Crystal field parameter
DWF	Debye-Waller Factor
E_g	Energy gap
H_{cs}	Electrostatic energy Hamiltonian
H_{so}	Spin orbit interaction Hamiltonian
IR	Infrared
LPVD	Laser Pulsed Vapor Deposition
PGHB	Photon-gated holeburning
PMMA	Polymethyl Methacrylate
PMT	Photomultiplier Tube
POGHB	Power-gated holeburning
RE	Rare Earth
SEM	Scanning Electron Microscopy
TEM	Tunneling Electron Microscopy
Ti-shapphire	Titanium Shapphire
TPA	Two-photon absorption
ZPL	Zero Phonon Line
cw	continuous wave
e_g	see Γ_3
t_{2g}	see Γ_5
Γ_3	4 Fold degenerate electronic state
Γ_5	6 Fold degenerate electronic state
Γ_{inh}	Inhomogeneous line width of transition
Γ_h	Homogeneous line width of transition
Γ_{hole}	Halfwidth of spectral hole

10. Publications

This section lists the published work carried out during the course of this project.

Patents

1. High Density and Fast Persistent Spectral Hole Burning in II-VI Compounds for Optical Data Storage (Status: U.S Pending)
2. II-VI Compounds as a Medium for Optical Data Storage Through Fast Persistent High Density Spectral Hole Burning (Status: Pending)

Doctoral Theses

The following Ph.D. theses are available from the Graduate Office Temple University.

1. Electro-Optical Properties of III-V Multiple Quantum Well Structures for Light Modulation at Visible Wavelengths, Submitted by *Milen Shiskov* to the Department of Physics, Temple University, Year: 1999, Current Address: Department of Physics, Harvard University, Cambridge MA.
2. Persistent Spectral Hole-burning in Europium and Europium Samarium Doped CaS, Submitted by *Mike Solonenko* to the Department of Physics, Temple University, Year: 1999, Current Address: Department of Physics, University of Pennsylvania, Philadelphia, PA.
3. High-Density Photon-Gated Hole-burning, Submitted by *Levent Biyikli* to the Department of Physics, Temple University, Year: 1999. Current Address: 3M Laboratories, Austin, Texas.

Refereed Publications

1. Spectral Hole-burning in MgS:Eu Nanoparticles, S. Dardona, L. Biyikli, R. Esposito and Z. Hasan, SPIE Proceedings on Three and Four-Dimensional Spectral Storage, Volume 4459, (2001).
2. Mechanism of High Density Power-Gated Hole-burning in Eu^{2+} -doped Sulfides, Z. Hasan and L. Biyikli, Journal of Optical Society of America B, 18, 232 (2001).

3. Thin Films of Sulfides for High Density Optical Storage by Photon-Gated Hole-burning, M.F. Aly, L. Biyikli, S. Dardona, J.L. Park and Z. Hasan, SPIE Proceedings on Photonic Devices and Algorithms for Computing, 4114, 182-188 (2000).
4. High Density Frequency Domain Storage in Alkaline Earth sulfides Double-Doped with Lanthanides, M.F. Aly, L. Biyikli, S. Dardona, and Z. Hasan, SPIE Proceedings on Photonic Devices and Algorithms for Computing, 4114, 262-268, (2000).
5. Photon-Gated Hole-burning Materials: Direction in High Density Memory Storage, Z. Hasan and L Biyikli, Materials Science Forum 315-317, 51-58 (1999) Invited Paper.
6. The Dynamics of Hole-burning in $4f^n-4f^n5d^1$ Transition of Eu^{2+} in MgS, L. Biyikli and Z. Hasan, J. Lumin. 83, 373-377, (1999).
7. Modulation of Visible Light by AIAs/AlGaAs Multiple Quantum Well p-i-n Structure, M. Shishkov, F. Karwacki, Z. Hasan and Jack E. Cunningham, IEEE, J. Quant. Elec. 35, 1176-1179 (1999).
8. Inhomogeneous Broadening and Gated Hole-burning in MgS:Eu and CaS:Eu in Polymethyl-methacrylate (PMMA), S. M. Syedahmedian, M.F. Aly, L Biyikli, J.L. Park, M. Solonenko, and Z. Hasan J. Lumin. 84, 389-392, (1999).
9. Pulsed Laser Deposited Thin Films of Sulfides for High Density Memory Storage, J.L. Park, L Biyikli, M.F. Aly, and Z. Hasan, SPIE Proceedings on *Advanced Optical Data Storage: Materials, Systems and Interfaces to Computers* Eds: Z. Hasan and P. Mitkas 3802, 206-212 (1999).
10. Persistent High Density Spectral Hole-burning in CaS:Eu and CaS:Eu, Sm Phosphors, Z. Hasan, M. Solonenko, P. I. Macfarlane, L. Biyikli, V. K. Mathur and F.A. Karwacki, App. Phys. Letters, 72, 2373-2375 (1998).

11. Power-Gated Spectral Hole-burning in an Unstable System (MgS: Eu²⁺, Eu³⁺): A Case for High Density Gated Hole-burning, Z. Hasan, L. Biyikli, and P. I. Macfarlane, *App. Phys. Letters*, 72, 3399-3401 (1998).
12. Material Challenges for Spectral Hole-burning Memories-, Z. Hasan, SPIE Proceedings on *Adv. Opt. Mem. and Interfaces to Computer Storage*, eds: P. Mitkas and Z. Hasan, 3468, 154-164 (1998).
13. Optical Biasing of a Ring Laser Gyroscope with a Quantum Well Mirror, F. A. Karwacki, M. Shishkov, Z. Hasan, M. Sanzari and H.L Cui, *Proc. IEEE Symposium on Position Guidance and Navigation Systems*, 161 1-8 (1998).
14. Novel High Frequency QW Optical Modulator Based on Surface Effects, F. Karwacki, H. L. Cui and M. Sanzari and Z. Hasan, SPIE Proceedings on *Curr. Develop. In Opt. Design and Eng.*, eds: R. Fisher and J. Smith, 3429, 117-22 (1998).
15. A Quantum Well Mirror: A Semiconductor Optical Biasing Element for a Ring Laser Gyroscope (RLG), F. A. Karwacki, M. Shishkov, Z. Hasan, M. Sanzari and H. L. Cui, 24th JSDE Conference, (1998).
16. High Density Photon-Gated Hole-burning in Sulfides, L. Biyikli, M. Solonenko, S.M. Ahmadyan and Z. Hasan, SPIE Proceedings on *Advanced Opt. Mem. and Interfaces to Computer Storage*, Eds: P. Mitkas and Z. Hasan, 3468, 285-292 (1998).
17. Energy Transfer and Upconversions in Cubic Cs₂NaYCl₆: Er³⁺ and Cs₂NaErCl₆, Z. Hasan, L. Biyikli, M. J. Sellars, G. A. Khodaparast and F. S. Richardson, *Physical Review B* 56, 4518-4528 (1997).

Publications in Advanced Stages of Preparation

1. Rare Earth Materials for Optical Storage (An invited review chapter in the *Hand Book of Rare Earths*, Springer Verlag, Germany)

2. Multiple Quantum Well Macro-Structures Designed for Visible Light Modulation, M. Shishkov F. Karwacki, M. Sanzari and Z. Hasan (to be submitted to Journal of Applied Physics).
3. Theoretical Aspects for Designing a Quantum Well Mirror, P. Zhao, H. Cui, M. Shishkov, F. Karwacki, Z. Hasan and M. Sanzari (to be submitted to JOSA).
4. Enhanced Inhomogeneous broadening and Photon Gated Hole-burning in Micro-particles of MgS:Eu and in CaS:Eu Polymethylmethacrylate (PMMA), Z. Hasan, L. Biyikli, M. Solonenko (to be submitted to App. Phys. Lett.).
5. Nanosecond High Density Photon Gate Hole-burning in MgS: Eu²⁺, Z. Hasan, and L. Biyikli (to be submitted to App. Phys. Lett.).
6. Photochemical and Photophysical Holeburning Processes in Rare Earth Doped MgS: Eu²⁺, Eu³⁺, L. Biyikli, P. I. Macfarlane and Z. Hasan (to be submitted to Phys. Rev. B.).
7. Photoionization induced Two Photon Spectral Hole-burning in the 4f-5d Transition of Eu²⁺ Doped CaS, M. Solonenko, P. M. Macfarlane and Z. Hasan (to be submitted to Phys. Rev. B).
8. The Mechanism of Persistent Spectral Hole-burning in Sulfides, Z. Hasan, L. Biyikli and J. Park (to be submitted to Optics Lett.).
9. MgS:Eu²⁺ - A New Standard for Materials for Optical Hole-burning Based Memory Storage, Z. Hasan and L. Biyikli (to be submitted to Optics Lett.).

Contributed Papers at Professional Meetings

1. Rare Earth Doped Nano-particles of MgS:Eu for Quantum Computing, PIERS Conference, Cambridge, July 2002.

2. Modulation of Visible Light by Macro-Structure Quantum Wells, M. Shishkov, F. Karwacki, Z. Hasan, Optical Society of America Meeting, Providence, Rhode Island, October 22-26, 2000.
3. A Tunable Multi-frequency VCSEL, Achieved by Using a Quantum Well Mirror, F. Karwacki, Z. Hasan, H. L. Cui, M. Sanzari, Optical Society of America Meeting, Providence, Rhode Island, October 22-26, 2000.
4. Multi-layer Thin Films of Rare Earth Doped II-VI Materials for High Density Optical Storage, M.F. Aly, L. Biyikli, S. Dardona, J.L. Park and Zameer Hasan, Optical Society of America Meeting Providence, Rhode Island, October 22-26, 2000.
5. High Density Frequency Domain Optical Storage Using Rare Earth Co-Doped II-VI Materials, M.F. Aly, L. Biyikli, S. Dardona and Zameer Hasan, Optical Society of America Meeting, Providence, Rhode Island, October 22-26, 2000.
6. Atomic Scale High-Density Spectral Memories, Z. Hasan, L. Biyikli and S. Dardona, Optical Society of America Meeting, Providence, Rhode Island, October 22-26, 2000.
7. Thin Films of Sulfides for High Density Optical Storage by Photon-Gated Hole-burning, M.F. Aly, L. Biyikli, S. Dardona, J.L. Park and Z. Hasan, SPIE Meeting on Photonic Devices and Algorithms for Computing, San Diego, July 3-7, 2000.
8. High Density Frequency Domain Storage in Alkaline Earth sulfides Double-Doped with Lanthanides, M.F. Aly, L. Biyikli, S. Dardona, and Z. Hasan, SPIE Meeting on Photonic Devices and Algorithms for Computing, San Diego, July 3-7, 2000.
9. High-Density Optical Storage in Thin Films of Sulfides by Photon Gated Hole-Burning, M.F. Aly, L. Biyikli, S. Dardona J.L. Park and Zameer Hasan, American Institute of Physics March Meeting Minneapolis, Minnessotta, March 21-25, 2000.

10. High-Density Frequency Domain Storage in Alkaline Earth Sulfides Double-Doped with Lanthanide, M.F. Aly, L. Biyikli, S.I. Dardona, Zameer Hasan, American Institute of Physics March Meeting Minneapolis, Minnessotta, March 21-25, 2000.
11. Macro-Structure Visible Light Quantum Well Modulator, Milen Shishov, Zameer Hasan, and Francis A. Karwacki, American Institute of Physics March Meeting Minneapolis, Minnessotta March 21-25, 2000
12. High Density and Fast Spectral Hole-burning In Thin Films of II-VI Materials Doped With Rare Earths, Z. Hasan, M.F.Aly, L.Biyikli, S. Dardonah and J.L. Park, 20th ONR Meeting on Physics of Quantum Electronics, Snow Bird, UT, Jan. 2000.
13. Macroscopic Multiple Quantum Well Modulators for ring Laser Gyroscopes, F. Karwacki, M. Shishkov and Z. Hasan, 20th ONR Meeting on Physics of Quantum Electronics, Snow Bird, UT, Jan. 2000.
14. Nanosecond Power-Gated Photo-ionization Hole-burning in $4f^7 - 4f^6 5d^1$ Transition of Eu^{2+} in II-VI Materials, L. Biyikli, M. Solonenko, Z. Hasan, Annual Meeting of the Optical Society of America, Santa Clara, Sept. 1999.
15. Pulsed Laser Vapor Deposited Thin Films of Sulfides as a Photon-Gated Hole-burning Material, J. Park, M. Aly, L. Biyikli, Z. Hasan, Annual Meeting of the Optical Society of America, Santa Clara, Sept. 1999.
16. High Temperature Photon-Gated Hole-burning in Sulfides, L. Biyikli, M. Solonenko, and Z. Hasan, Annual Meeting of the Optical Society of America, Santa Clara, September. 1999.
17. The Dynamics of Hole-burning in $4f^n - 4f^{n-1} 5d^1$ Transition of Eu^{2+} in MgS, L. Biyikli and Z. Hasan, International Conference on the Dynamical Processes in the Excited State of the Condensed Matter, DPC 99, San Juan Puerto Rico, August 1999.

18. Hole-burning in MgS: Eu and CaS: Eu in Polymethylmethacralate [PMMA], S. M. Ahmedyan, M. Aly, L. Biyikli, J. Park, M. Solonenko and Z. Hasan, International Conference on the Dynamical Processes in the Excited State of the Cond. Matter DPC 99, San Juan Puerto Rico, August 1999.
19. The Dynamics of Hole-burning in MgS, L. Biyikli and Z. Hasan, Workshop on Applications of Spectral Hole-burning, Bozeman, March 7-10, 1999.
20. Inhomogeneous Broadening and Hole-burning in MgS: Eu and CaS: Eu in Polymethylmethacralate [PMMA], S. M. Ahmedyan, M. Aly, L. Biyikli, J. Park, M. Solonenko and Z. Hasan, Workshop on Applications of Spectral Hole-burning, Bozeman, March 7-10, 1999.
21. The Effect of Pressure on the Hole-burning Properties of Eu^{2+} in Polycrystalline Sulfide Samples, M. Aly, L. Biyikli, and Z. Hasan, Workshop on Application of Spectral Hole-burning, Bozeman, March 7-10, 1999.
22. Modulation of Visible Light by AlAs/AlGaAs Multiple Quantum Well p-i-n Structures, M. Shishkov, Z. Hasan, and F. Karwacki, OSA Meeting, Baltimore, Oct. 1998.
23. Enhanced Inhomogeneous Broadening and High Density Gated Spectral Hole-burning in MgS:Eu and CaS:Eu Particles in Polymethylmethacralate (PMMA), L. Biyikli, M. Solonenko, J. Park, S. M. Ahmedyan, M. Aly and Z. Hasan, OSA Meeting, Baltimore, Oct. 1998.
24. Photon Gated Hole-burning in MgS: Eu^{2+} , Z. Hasan and L. Biyikli, OSA Meeting, Baltimore, Oct. 1998.
25. Photon Gated Hole-burning in MgS: Eu^{2+} , L. Biyikli, P. Macfarlane and Z. Hasan, Workshop on Applications of Spectral Hole-burning, held at Montana State University, Bozeman, March 7-9, 1998.

26. Photospectral Hole-burning in Ca: Eu and Eu, Sm Phosphors, M. Solonenko, L. Biyikli, P. Macfarlane and Z. Hasan, APS March Meeting Los Angeles, March 16-20, 1998.
27. High Density Photospectral Hole-burning using Photoionizable Centers of Rare Earths in MgS, L. Biyikli, P. Macfarlane and Z. Hasan APS March Meeting Los Angeles, March 16-20, 1998.
28. Phase Modulation of Visible Light in AlAs/Al GaAs Multiple Quantum Well Structures, M. Shishkov, Z. Hasan and F. Karwacki, APS March Meeting Los Angeles, March 16-20, 1998.

11. Index

- II-VI materials doubly doped with rare earths, **5.7**
- absorption, emission and excitation setup, **4.6.1**
- $\text{Al}_2\text{O}_3:\text{Ti}^{3+}$, **5.8**
- background and experimental methods, **4**
- conclusion, **6**
- cryogenics, **4.7**
- electronic transitions in rare earth for high-density storage, **4.3.2**
- experimental procedures for optical studies, **4.6**
- fast optical erasure, **5.1.5**
- fast writing, **5.1**
- high density holeburning in $\text{MgS}:\text{Eu}$ in polymers (PMMA), **5.4.1**
- high efficiency of holeburning, **5.1.2**
- high -resolution optical holeburning setup, **4.6.3**
- high temperature cycling and storage of data, **5.1.4**
- holeburning
 - in $\text{MgS}:\text{Eu},\text{Ce}$, **5.7.2**
 - in $\text{MgS}:\text{Eu},\text{Sm}$, **5.7.1**
 - in nanoparticles, **5.5**
- homogeneous and inhomogeneous broadening in solids, **4.1**
- introduction, **3**
- low photon budget, **5.1.6**
- material,
 - characterization, **4.5**
 - designing and processing, **4.4**
 - selection, **4.3**
- mechanism of holeburning, **5.1.1**
- $\text{MgS}:\text{Eu}$ embedded in different hosts, **5.4**
- microparticles of RE doped of II-VI sulfides, **4.4.1**
- Mössbauer studies, **5.3**
 - of $\text{Eu}^{2+}/\text{Eu}^{3+}$ based materials, **4.5.1**
- multi-layer thin film fabrication (LPVD), **4.4.4.3**
- nanoparticles by quench condensation of laser ablated vapors, **4.4.4**
- optical characterization, **4.5.2**
- photon-gated and power-gated holeburnings, **4.2**
- recommendation, **7**
- references, **8**
- results, **5**
- structural properties, **4.3.1**
- summary, **1**
- symbols, abbreviations, acronyms, **9**
- temperature dependence, **5.1.7**
 - in different hosts, **5.6**
- theoretical estimate of 5d- energy levels, **4.3.3**
- thin film and multi-layer structures, **4.4.2**
- ultra-high density storage
 - in $\text{MgS}:\text{Eu}^{2+}$, **5.1**
 - in multi-layer, multi-center structures, **5.2.1**
 - in thin films, **5.2**